Australian Government
Geoscience Australia

Professional Opinion

No. 2009/02

CONSULTANCY REPORT

A Probabilistic Tsunami Hazard Assessment of the Southwest Pacific Nations

Thomas, C. and Burbidge, D.

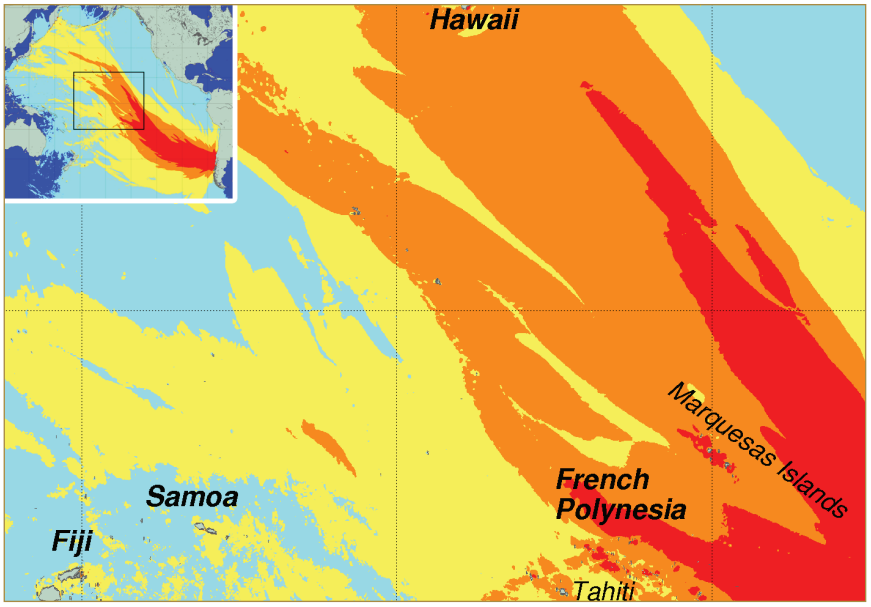

PREPARED FOR:

AusAID

February 2009

Department of Resources, Energy and Tourism
Minister for Resources and Energy: The Hon. Martin Ferguson, AM MP
Secretary: Mr Drew Clarke

Geoscience Australia
Chief Executive Officer: Dr Chris Pigram

GeoCat # 68193

Bibliographic reference: Thomas, C. and Burbridge, D. 2009. A Probabilistic Tsunami Hazard Assessment of the Southwest Pacific Nations. *Geoscience Australia Professional Opinion. No.2009/02*. Re-released in 2011.

Contents

1 Executive Summary

The Indian Ocean tsunami of December 26, 2004 and subsequent smaller events (off Nias in 2005, Java in 2006 and the Solomon Islands in 2007) have increased awareness among emergency management authorities throughout the Pacific of the need for more information regarding the hazard faced by Pacific nations from tsunami. Over the last few years the Australian Government has undertaken an effort to support regional and national efforts in the southwest Pacific to build capacity to respond to seismic and tsunami information. As part of this effort, Geoscience Australia has received support from AusAid to partner with the South Pacific Applied Geoscience Commission (SOPAC) to assist Pacific countries in assessing the tsunami hazard faced by nations in the southwest Pacific.

The tsunami threat faced by Pacific island countries consists of a complex mix of tsunami from local, regional and distant sources, whose effects at any particular location in the southwest Pacific are highly dependent on variations in seafloor shape between the source and the affected area. These factors make the design of an effective warning system for the southwest Pacific problematic, because so many scenarios are possible and each scenario's impact on different islands is so varied. In order to provide national governments in the southwest Pacific with the information they need to make informed decisions about tsunami mitigation measures, including development of a warning system, a comprehensive hazard and risk assessment is called for.

The aim of the report is to provide a *probabilistic tsunami hazard assessment* (PTHA) to SOPAC and AusAID to quantify the expected hazard for the SW Pacific nations. It follows a preliminary report of the tsunami hazard (Thomas et al, 2007) that was restricted to maximum credible tsunami events. In this report, the hazard will be reported in terms of:

- tsunami amplitudes[1] at locations offshore the nations included in this study, and
- the probabilities of experiencing these amplitudes.

1.1 Scope

The following nations were included in the study (Figure 1) :

American Samoa	Cook Islands
Fiji	Federated States of Micronesia
French Polynesia	Guam
Kiribati	Marshall Islands
Nauru	New Caledonia
Niue	Palau
Papua New Guinea	Samoa
Solomon Islands	Tokelau
Tonga	Tuvalu
Vanuatu	

[1] Throughout this report the term *amplitude* is used to denote the wave height from mean sea level to crest.

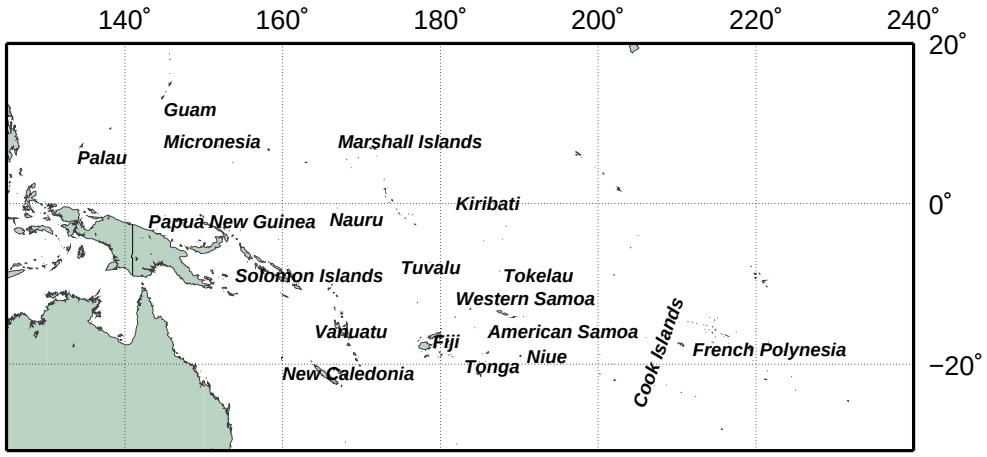

Figure 1: SOPAC nations included in the study.

The study focused on tsunami caused by earthquakes and, more particularly, earthquakes occurring in subduction zones. While tsunami can be caused by other types of earthquakes, as well as asteroid impacts, landslides and volcanic collapses and eruptions, earthquakes in subduction zones are by far the most frequent source of large tsunami, and are therefore the only events considered here. The subduction zones included in this study are limited to those that could credibly impact on the SOPAC nations (i.e. all those around the Pacific Rim).

Tsunami hazard in this report is expressed as the *annual exceedence probability* of a tsunami exceeding a given amplitude at a given offshore depth. An alternative way of expressing the annual probability is as a *return period*. The return period is the average length of time expected between events exceeding a given amplitude at a given offshore depth. The offshore depth in this assessment was chosen to be 100m. The main reason for choosing this depth was because modelling amplitudes to shallow water depths is a more computationally intensive task that requires higher resolution bathymetric data which does not exist for all regions considered in this study.

The quality and resolution of the bathymetric dataset used is one of the factors that limits the accuracy of modelled tsunami amplitudes. While the resolution used in this study (two arc minutes, ≈ 3.7 kilometres) is considered sufficient for the modelling of tsunami in deep water in the open ocean, in regions of very complex bathymetry close to shore the results must be interpreted with caution. This highlights the need for more detailed studies in some regions, using higher resolution bathymetric data. Another consequence of the resolution of the bathymetry data used is that there may be some very small inhabited islands in the study region that are not represented as islands by the bathymetry, and therefore may not be represented in the study. These issues are discussed in more detail in Section A.2 of the Appendix.

It is important to emphasise that the results of this investigation cannot be used directly to infer onshore inundation, run-ups or damage. Such phenomena are strongly dependent not only on the offshore tsunami height, but also on factors such as shallow bathymetry and onshore topography. A study of inundation therefore requires detailed bathymetric and topographic data and involves even more intensive numerical computations than those required for this study. The object of this assessment is to answer the broader question: which Pacific nations might experience offshore amplitudes large enough to potentially result in hazardous inundation, what are the probabilities of experiencing these amplitudes, and from which subduction zones might these tsunami originate? This

information can be used to inform more detailed inundations studies.

1.2 Method

The method used in this investigation may be summarised thus:

- Determine the earthquake source zones to be included in the study (Figure 5 and the discussion in Section A.4 of the Appendix).
- For each source zone, determine the possible characteristics of the earthquakes that could occur in that source zone, and the probability of each such earthquake occurring, and assemble a large catalogue of possible earthquakes.
- Simulate the possible earthquakes and, for each nation in the study, estimate the maximum tsunami amplitudes that result from each event in the catalogue of earthquakes at a number of selected locations (called *model output points*) near that nation. (See Figure 2 for the location of all the model output points used in the study.)
- Combine these results to relate maximum tsunami amplitudes to the probabilities that they might occur.

An assumed maximum earthquake magnitude was assigned to each source zone and possible events having magnitudes from 7.0 to the maximum (in increments of 0.1) and with various characteristics were simulated. A total of 59,871 simulated (or *synthetic*) earthquakes were included. Probabilities were assigned to each of these events using the historical record and the available geophysical information, however the uncertainties in assigning these probabilities increase with earthquake magnitude. Details of this methodology are outlined in the Appendix.

Numerical computations were performed to simulate the propagation of tsunami waves from the earthquake source zones to the model output points. The results of these simulations were used to estimate the maximum tsunami amplitude at each model output point due to each synthetic earthquake. The resulting data may be mapped in various ways to give a visual representation of the hazard faced by each of the nations, and the sources of that hazard.

1.3 The Hazard Maps

In this report the results of the study are presented with the aid of the following types of diagrams:

1. **Hazard Curves:** These describe the relationship between the return period and the maximum tsunami amplitude for a particular model output point. The tsunami amplitude given on the y-axis is predicted to be exceeded with the average return period given by the x-axis. In Section 3, which describes the results for each countries, hazard curves are shown as part (a) in the figure within each countries' section. For example, Figure 6(a) shows the hazard curves for all the points offshore American Samoa.
2. **Maximum Amplitude Maps:** The maximum tsunami amplitude that will be exceeded at a given return period for every model output point in a region. A

different map for the region can be drawn for each return period. Figure 2 is an example of such a map drawn for the 2000 year return period for the whole region. In Section 3, these maps form part (c) of each countries' respective figure.

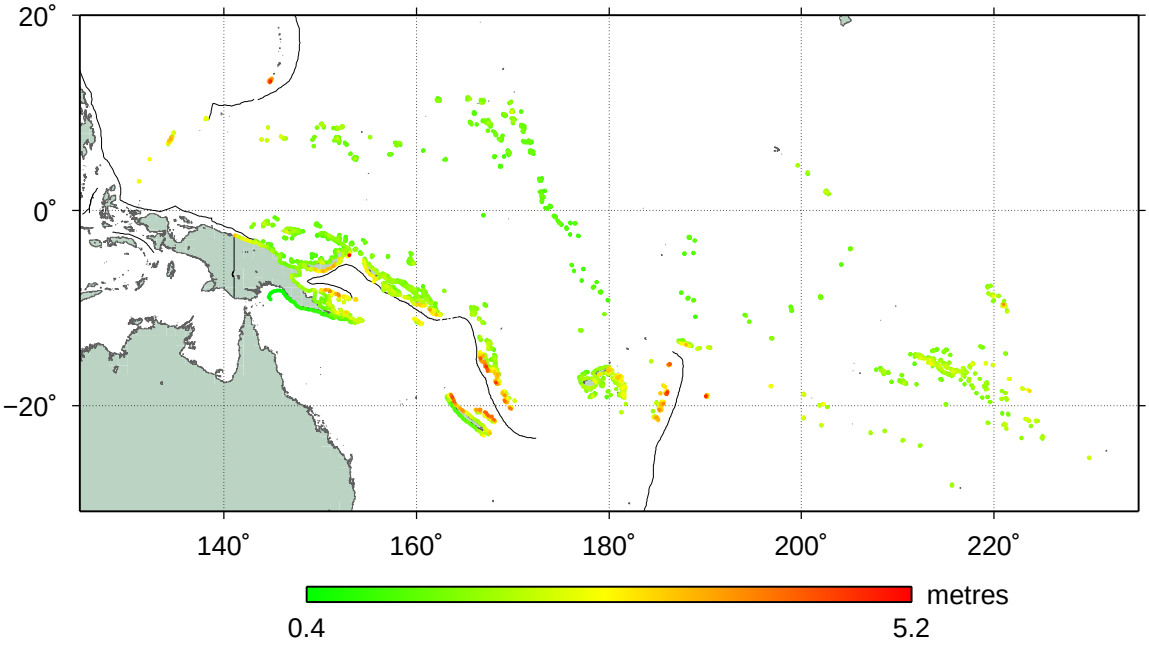

Figure 2: Maximum amplitude for a 2000 year return period for all model output points in the study. Black lines show the subduction zones included in this study in the area covered by the map.

3. **Probability of Exceedance Maps:** For a given amplitude, these maps show the annual probability of that amplitude being exceeded at each model output point in a region. A different map can be drawn for each amplitude for that region. The KML files beginning with "probability_of_exceedence" on the accompaning DVD are examples of this kind of hazard map, see Section 1.3.1 for details. Figure 3 is an example screenshot of this type of map.

4. **Deaggregated Hazard Maps:** These indicate the relative contribution of different source zones to the hazard *at a single location.* A different map will be obtained for every choice of model output point (and for different return periods), and so there are a great many possible deaggregated hazard maps that may be drawn for any given region. Examples of deaggreagted hazard maps can be found on the DVD (see Section 1.3.1).

5. **Regional Weighted Deaggregated Hazard Maps:** These give an indication of the source of the hazard to a nation or region as a whole, and are are not specific to a particular offshore location. While regional weighted deaggregated hazard maps provide a convenient summary of the source of hazard over a region, if one is interested in the hazard at a particular location, near a large town for example, then one should consult a deaggregated hazard map for a model output point near that particular location. Part (b) of the figures shown in Section 3 are examples of this type of hazard map.

More details are given about the method of producing the deaggregated and regional weighted deaggregated hazard maps in Section A.7 of the Appendix.

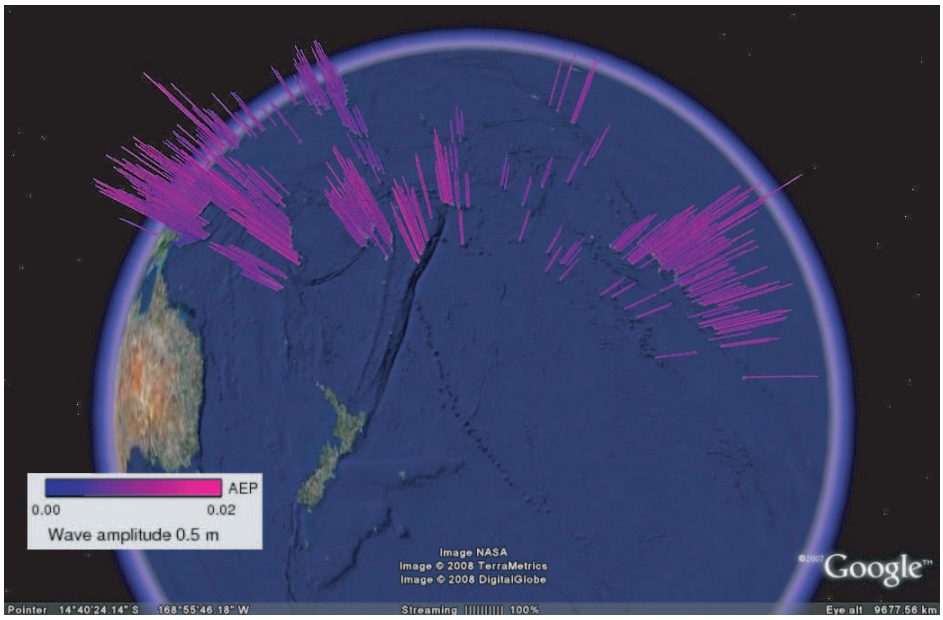

Figure 3: Probability of a tsunami exceeding a maximum tsunami amplitude of 0.5m for the offshore points considered in this assessment. This is a screenshot of one of the KML maps included on the DVD.

1.3.1 KML Files on the Companion DVD

It is possible to draw many more maps than sensibly can be placed in a report such as this. Moreover, diagrams of types 2 to 5 above are very well suited to being presented using Google Earth^{TM}. Accordingly, there is a companion DVD containing KML files that, when imported into Google Earth^{TM}(or similar mapping software), give a very good representation of these maps. Each KML file produces a collection of coloured columns showing the relative values of a dataset from the PTHA. The height and colour of the columns reflect the values of the data being represented, and the map can be interrogated by clicking on the small dot on the top of each column, which will display the value represented by that column.

The KML dataset is divided into three categories:

1. Files with names of the form "probability_of_exceedance_x.kml" show our estimates of the annual probability of the maximum amplitude of a tsunami exceeding "x" meters at approximately the 100m contour. For example, the file "probability_of_exceedance_1.0.kml" is the annual probability of a wave exceeding 1.0m at the locations of the bars. This dataset allows the user to determine how often a wave could be expected to exceed a specific amplitude of interest (eg one metre). If there is a specific amplitude at which a certain response is required, then these maps can tell the user the probability of that response being needed per annum for that location offshore. Figure 3 is an example of this type of map.

2. KML files with names of the form "wave_amplitude_x.kml" on the DVD show the maximum tsunami amplitude that can be expected to be exceeded every "x" years. For example, "wave_amplitude_1000.kml" is a map showing the maximum wave amplitude with a 1 in 1000 year chance of being exceeded at the locations of the bars. This is an alternative way of plotting the hazard where the probability is fixed and the amplitude is plotted, instead of fixing the amplitude and plotting the annual

probability. This functionality allows the user to determine the maximum "1 in x year wave amplitude" for a particular offshore location. Waves with an amplitude greater than this number therefore only happen less often than 1 in "x" years.

3. The KML files with deaggregated maps have filenames of the form "deaggregation-i_lonx_laty_z.kml". This shows the deaggregated hazard for location "i" (a numerical location id) at longitude "x" and latitude "y" with return period "z". These maps show the percentage of the annual probability of exceedance at a specific return period which results from each sub-fault. This value varies depending on the specific location off the coast chosen for the deaggregation. These maps allow the user to determine which zones are the most important for a given location at a given return period (e.g. they may wish to know which zones can contribute to the 1 in 2000 year wave for a particular section of coast). Generally the smaller wave amplitudes (or equivalently shorter return periods) come from a wider range of possible sources. Conversely, the larger wave amplitudes (or equivalently longer return periods) come from a more restricted range of possible sources, usually from a fault that is ideally located to direct large waves to that location. The deaggregation location (x, y) is indicated on the map by a white square with zero height. Google Earth will zoom into this square when the dataset is loaded.

The probability_of_exceedance and wave_amplitude files are located in the subdirectory hazard_maps while the deaggregation files are in the subdirectory deaggregations.

1.4 Summary of Results

The results are discussed by nation in Section 3, and are presented in detail graphically in the KML files on the accompanying DVD. Here we give an overview of the results for the region as a whole.

Table 1 shows the tsunami amplitude that has a 1 in 2000 year chance of being exceeded for each SOPAC nation. Nations in red have the highest hazard at this return period (Guam, New Caledonia, Niue, PNG, Tonga and Vanuatu), while those in green have the least (Nauru and Tuvalu). The other SOPAC nations are distributed between these two more extreme groups.

Figure 2 shows the maximum amplitudes at the model output points for a return period of 2000 years, along with those faults included in the study that lie in the mapped region. It is clear from Figure 2 that most of the nations in the highest category mentioned above lie very close to subduction zones. Typically where a nation is close to a subduction zone (the black lines in Figure 2) the bulk of the hazard to that nation comes from that zone. It should also be noted, that when an earthquake is that close to country, there is unlikely to be enough time for an alert to reach that country from centralised warning centres such as the Pacific Tsunami Warning Centre. Therefore public awareness campaigns are one of the best ways to reduce the hazard from such a local source.

When the nation is not close to any particular zone the hazard usually comes from a wider range of possible sources and is usually lower because the extra distance reduces the amplitude of the tsunami by the time it reaches the nation concerned. These nations typically have a more moderate hazard (e.g. French Polynesia). There would also be more time for a warning from organisations such as the PTWC to reach those countries. Some nations (eg Nauru and Tuvalu) are not located optimally for any zone to send a tsunami towards them and they thus experience relatively low tsunami hazard. Since some of

SOPAC nation	1 in 2000yr tsunami amplitude (m)	Most Important Subduction Zones
American Samoa	2.3	Tonga
Cook Islands	2.7	Tonga
Fiji	3.3	Tonga, New Hebrides
French Polynesia	3.8	(Society Is) Tonga, Peru, Chile, Kurils (Marquesas Is) Chile, Peru, Aleutians (Acteon Grp) Tonga, Kermadec, Peru, Chile, Aleutians (Austral Is) Tonga, Peru, Chile (Tuamotu Arch) Tonga, Peru, Chile, Kurils, Mid-America, Aluetians
Guam	4.9	Mariana, Phillippines
Kiribati	2.2	(Gilbert Is) Kurils, New Hebrides, Mariana, Aleutians, Peru, Chile, Tonga (Phoenix Is) Kurils, New Hebrides, Chile, Tonga (Line Is) Kurils, Chile, Peru, Tonga, Mariana, Aleutians
Marshall Islands	2.5	Kurils, Mariana, Tyukyu, New Hebrides, Phillipines, Chile
F.S. of Micronesia	2.6	(Yap) Phillipines, Mariana, New Guinea. (Chuuk) Mariana, Philipines, Ryukyu, Kurils, Aleutians. (Pohnpei) Mariana, Phillipines, Kurils, Ryukyu, Nankai, Aleutians.
Nauru	1.0	Mariana, Phillippines, Columbia, Peru, Chile, Kermadec, Aleutians
New Caledonia	4.5	New Hebrides, Kermadec, Solomons
Niue	4.8	Tonga
Palau	3.5	Philippines, New Guinea
Papua New Guinea	5.2	(New Britain) Solomons (Mainland) New Guinea, Solomons, New Hebrides, Phillipines, Mariana
Samoa	3.4	Tonga
Solomon Islands	3.4	Solomons, New Hebrides
Tokelau	1.4	New Hebrides, Tonga, Kurils, Peru, Chile
Tonga	4.7	Tonga
Tuvalu	1.6	New Hebrides, Tonga
Vanuatu	4.7	New Hebrides, Kermadec

Table 1: Summary of results. The second column shows the maximum tsunami amplitude with a 1 in 2000 year chance of being exceeded for any point off the SOPAC nation shown in the first column. The nations shown in red have the highest (greater than 4m maximum tsunami amplitude) hazard at this return period. The nations shown in green have the lowest (tsunami amplitude is less than 2m) at this return period. The third column lists the subduction zones which contribute the most to the 1 in 2000 year hazard for that nation. Nations which cover a large area are split into different regions. The location of the region is indicated by the major island in the region given in brackets.

the SOPAC nations are very spread out over the Pacific, the zones which are the most important to that nation can vary significantly for different parts of the country. For a more detailed discussion for the hazard for each country, please see Section 3.

It is also important to emphasise that whether the *risk* (likelihood of damage or death) from a tsunami also depends on the density of infrastructure in low lying areas exposed to tsunami attack and the amount of warning received and the responses to it. For some countries, even if the tsunami hazard offshore is fairly low, the consequences of the event could potentially be high. Only more detailed modelling and analysis of each specific island could determine whether this indeed the case for any of the countries covered by this report.

The other factor to bear in mind, is that the earthquake recurrence model used in this assessment takes the return periods of smaller magnitude earthquakes that have occurred historically and extrapolates this to longer return periods to estimate the return period of much larger earthquakes that haven't happend historically. Therefore there is much more uncertainity in the hazard estimates at the longer return periods. Additional data, particularly palaeo-tsunami data, is required to reduce the uncertainity in the hazard estimates given here for the longer return periods. This uncertainity would be the largest for countries whose main source of hazard comes from a zone which has not experienced a very large earthquake in the historic or known pre-historic catalogue. One example of this would be the Mariana's subduction zone which has not experienced an earthquake larger than 7.0-7.5 since 1900. The Mariana zone is an important source of hazard to islands such as Guam.

1.5 Glossary

Amplitude	Height of the crest of the tsunami wave above mean sea level.
Bathymetry	The measurement of the depth of the ocean floor from the water surface.
Probabilistic Tsunami Hazard Map	This map shows the wave amplitude around the coast that has a particular chance of being exceeded per annum. The larger the wave amplitude, the greater the hazard.
Run-up height	The maximum water elevation within the limit of inundation. It is usually greater than the wave amplitude at the coast.
Subduction zone	A region of the earth where two tectonic plates are converging and one plate is sliding beneath the other. One example is the Sunda Arc that stretches from Timor to Burma.
Topography	The measurement of the elevation of the land surface from sea level.
Tsunami	A wave created by a sudden disturbance of water. It is fast moving and has a small amplitude in deep water, but slows down and increases in height as it reaches shallow water.
Tsunamigenic	Capable of producing a tsunami.

2 Introduction to Tsunami

Tsunami are caused when large masses of water in the ocean are suddenly displaced by some event. Gravity acts to return the displaced water to its equilibrium position and the disturbance propagates as a wave, possibly for a very long distance. They differ from wind generated waves in that their wavelengths (distance from peak to peak) are very large, exceeding 100 kilometres in the open ocean, they involve movement of the water all the way to the ocean floor, and they travel very quickly, of the order of 600 to 700 kilometres per hour or more in deep water. Even very significant tsunami will have amplitudes of only a few tens of centimetres in deep water and are likely to pass unnoticed by the occupants of a boat. However they carry a great deal of energy and they are able to transport this energy very long distances. When these waves reach shallow water they slow down and "bunch up" (their wavelength decreases), and their height increases dramatically, a process known as *shoaling*. The maximum amplitude of the 2004 Boxing Day event was estimated to be around 0.6 metres in the open ocean (Song *et al*, 2005) but the tsunami ran up to heights of ten metres along many coasts, even those thousands of kilometres from the earthquake (for example in India, see Narayan *et al* 2005).

The most common causes of tsunami are large earthquakes occurring under the sea floor, when the sudden movement of large slabs of rock causes the overlying column of water to be displaced. Submarine landslides also cause tsunami, when sediment on steep slopes becomes unstable and fails under gravity, displacing a large volume of water. Less common are tsunami caused by the explosion or collapse of a volcano. Asteroids and comets may also generate tsunami if they fall into the ocean and, although such events are rare, there is evidence that tsunami generated by this mechanism may have reached Australia in prehistoric times (Bryant, 2001).

2.1 Earthquake Sources

The most common causes of tsunami are earthquakes along oceanic subduction zones. Subduction zones occur where two tectonic plates are colliding, and one of the plates is sliding (subducting) beneath the other (Figure 4). As this happens friction between the two

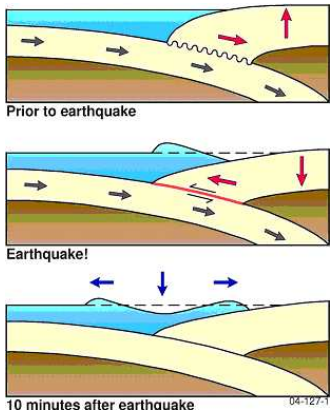

Figure 4: Mechanism for tsunami generation in an oceanic subduction zone.

plates may cause the upper plate to stick to the subducting plate and to become distorted by its motion. Eventually the stress associated with this deformation accumulates to such an extent that it can no longer be sustained by the frictional force between the plates, resulting in a sudden movement of the upper plate as it springs back into place. This is

known as a subduction zone earthquake. This movement causes a sudden displacement of the water lying above the plate, producing a tsunami. Not all earthquakes occur in subduction zones, and other types of earthquakes have been responsible for generating tsunami. However subduction zones have the potential to produce the largest earthquakes and the most significant tsunami. For this reason this study focuses exclusively on the oceanic subduction zones that could produce tsunami which impact on the area of interest.

The southwest Pacific area is surrounded by the "Ring of Fire", a region of intense tectonic activity. Numerous volcanoes ring the Pacific Ocean and it is the location of some of the largest and most seismically active faults in the world. Until the 2004 Indian Ocean tsunami it was also the location of some of the most damaging tsunami in recent history, such as the 1960 Chile tsunami and the 1998 Aitape tsunami (in the Sandaun province on the north coast of Papua New Guinea). Figure 5 shows the known plate margins in the Pacific coloured according to type. Subduction zone plate margins (shaded blue in Figure 5) are known to be the source of most of the largest earthquakes in history. The 1960 Chile tsunami was caused by a magnitude 9.5 earthquake along the subduction zone off the Chilean coast (ChT in Figure 5). The resulting tsunami caused major damage and deaths as far away as Hawaii and Japan and minor damage was reported throughout the Pacific (Alport and Blong, 1995). The USGS estimate of the death toll from this event is more than 2000, including 61 deaths in Hawaii, 128 deaths in Japan and 32 dead or missing in the Phillipines. For more information about this event, see Appendix C. The South American subduction zone has a long history of hosting large, tsunamigenic earthquakes and it will almost certainly continue do so in the future.

The southwest part of the Ring of Fire has also been known to produce large, tsunamigenic earthquakes, although none so far has been as large as the 1960 Chile earthquake. An earthquake, probably combined with a submarine landslide, produced the 1998 Aitape tsunami, which was the most lethal tsunami in this area in historic times. The earthquake probably occured along or near the New Guinea Trench to the north of PNG (labelled "NGT" in Figure 5). The Aitape tsunami devastated several villages in Papua New Guinea and killed 2200 people.

The subduction zone to the east of PNG near the Solomons Islands ("SST" and neighbouring zones in Figure 5) has also been known to produce large earthquakes. In April 2007 an earthquake of magnitude 8.1 occurred to the southwest of the Solomon Islands, near the South Solomon Trench (SST) subduction zone. The earthquake and resulting tsunami caused substantial damage and scores of deaths in the Solomon Islands. There have also been some unconfirmed reports of damage in Papua New Guinea from this event.

Further to the east and south of the Solomons, the subduction zone near the New Hebrides Trench (NHT in Figure 5) off Vanuatu is another plausible site for a great (magnitude greater than 8) tsunamigenic earthquake. The history of the tectonic uplift of this area, as preserved in coral growth bands, suggests that only moderate earthquakes (less than magnitude 8) have occurred along short segments of this subduction zone so far (Taylor *et al*, 1990). However, the potential for these segments of the Vanuatu subduction zone to rupture together in a single, very large, earthquake should not be discounted.

Further to the east and south again, the Tonga-Kermadec Trench subduction zones ("TnT" and "KmT" in Figure 5), stretching from the Tonga Islands to New Zealand, has historically experienced earthquakes of magnitude 8.0 to 8.3 which have generated local tsunami. Recent work on an earthquake that occurred in 1865, however, suggests that the potential for the generation of far-field tsunami in the Tonga-Kermadec Trench may have

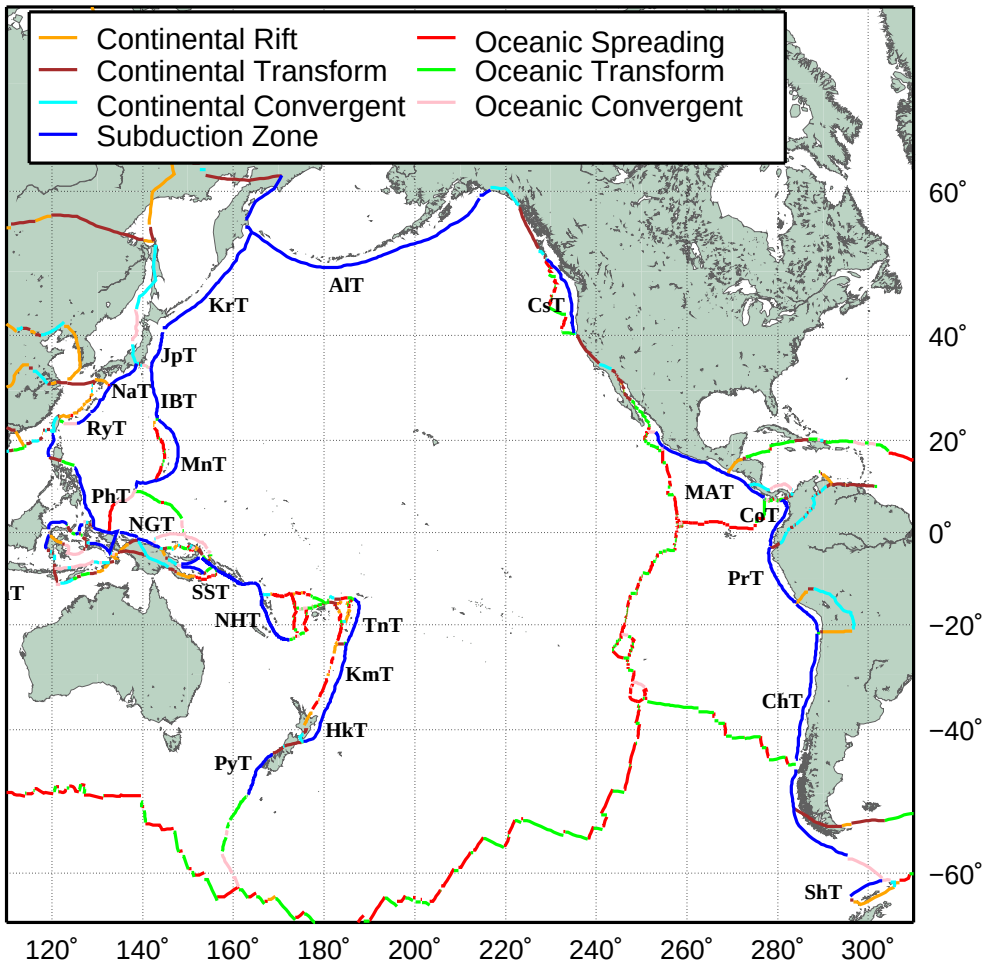

Figure 5: Map of major plate boundaries from Bird (2002). All subductions zones shown (in blue) were included in the study, and are labelled: AlT - Aleutian Trench, ChT - Chile Trench, CoT - Columbia Trench, CsT - Cascadia Trough, HkT - Hikurangi Trough, IBT - Izu-Bonin Trench, JpT - Japan Trench, KmT - Kermadec Trench, KrT - Kuril Trench, MnT - Mariana Trench, MAT - Middle America Trench, NaT - Nankai Trough, NGT - New Guinea Trench, NHT - New Hebrides Trench, PhT - Philippines Trench, PrT - Peru Trench, PyT - Puysegur Trench, RyT - Ryukyu Trench, SaT - South Sandwich Trench, SST - South Solomons Trench, TnT - Tonga Trench.

been underestimated (Okal *et al*, 2004).

South of New Zealand, much of the relative plate motion is in the strike direction (that is, in the direction of the fault line), so that even when large earthquakes occur the vertical component of the slip is small and they typically generate only small tsunami. There is, however, a section of plate boundary just to the south of New Zealand known as the Puysegur Trench ("PyT" in Figure 5), along which subduction has been occurring for the past ten million years, a very short time in geologic terms (Meckel *et al*, 2005). Subduction zones with such short histories are rare and their potential to produce large earthquakes and tsunami is unknown. No major tsunamigenic earthquake has occurred on this trench in the historic past (greater than magnitude 8), which would suggest either that subduction is mostly aseismic and no large earthquakes will occur, or that the subduction zone has been accumulating strain energy for over 200 years and has the potential to rupture in a major earthquake. However, the magnitude 7.4 earthquake along the Puysegur zone in September 2007 did create a small tsunami which was detectable by a deep ocean pressure gauge just off the fault (Bathgate *et al*, 2008).

In the north Pacific, the subduction zone off Cascadia ("CsT" in Figure 5) is thought to have hosted an earthquake around magnitude 9 in 1700 which generated a large tsunami that impacted Japan (Atwater *et al*, 2005). More recently, large earthquakes along the Aleutian Islands subduction zone ("AlT" in Figure 5) have generated waves that were damaging as far as Hawaii. The 1964 Prince William Sound earthquake (magnitude 9.2) created a damaging tsunami in Alaska. According to the USGS, that event took 125 lives (110 from the tsunami and 15 from the earthquake). There were also tsunamigenic events in 1965 (the magnitude 8.7 Rat Islands earthquake) and 1957 (the magnitude 8.6 Andreanof Islands earthquake). Both were large enough to create damaging tsunami in the Alaskan region.

Japan has a record of seismicity going back nearly one thousand years from the subduction zones off its coast. Events along the Nankai ("NaT") and Kamchatka-Kurils zones ("KrT") are known to create very large local tsunami, but as yet this area has not experienced any earthquake that we can be confident had a magnitude of 9 or above.

In summary, there are major subduction zones in the west, north and east of the Pacific Ocean basin that either have produced damaging tsunami in the past or could plausibly produce them in the future. Therefore there is a real prospect that any of the nations in the southwest Pacific might be exposed to a significant tsunami hazard.

2.1.1 Other Tsunamigenic Mechanisms

Subduction zone earthquakes are not the only possible sources of tsunami. As mentioned above, the Pacific is rimmed with volcanoes, many of which are submarine or near the coast. Should one of these volcanoes erupt violently or collapse suddenly into the sea, there is a real prospect of it producing a tsunami. For example, in 1888 a large tsunami, caused by the flank collapse of Mount Ritter in Papua New Guinea, ran up to 12 – 15 metres and wiped out villages on the western coast of New Britain (Johnson, 1987). The probability of this occurring is difficult to estimate without detailed study of the volcanoes concerned and may be a topic for future work.

The Aitape tsunami demonstrated that there is also the prospect of a landslide source generating a tsunami. The largest tsunami in history occurred in 1958 when an earthquake triggered a landslide into the Lituya Bay fjord in Alaska. The tsunami reached an altitude of 510 metres on the other side of the bay (Mader, 2002). However, tsunami generated in fjords usually remain trapped within them and are rarely considered to be a major threat outside of the local region.

Submarine landslides on the continental slope are also a genuine hazard. These can be triggered by a nearby earthquake, or may happen without warning. Historically they have tended to produce large, but local tsunami (for example the 1998 Aitape and 1953 Suva tsunami) but there is the prospect of a major tsunami that impacts the far-field if the landslide is sufficiently large. Again, this may be a topic for future work.

The largest tsunami of all are likely to be generated by asteroid impacts. It is known that major extinction events marking the transitions between geologic eras, such as that between the Cretaceous and Tertiary periods 65 million years ago, are the result of massive impacts of comets or asteroids of about ten kilometres in diameter. Objects capable of causing worldwide catastrophes are most certainly associated with massive tsunami, with wave amplitudes far exceeding any tsunami in historic times. There is considerable uncertainty about the generation and propagation of tsunami waves from intermediate-

sized objects with diameters in the range 100 metres to one kilometre. Smaller objects almost certainly do not generate tsunami. Larger objects are clearly capable of penetrating to the ocean floor and generating long-period waves that travel across the ocean with little loss of energy. These are likely to be quite rare, but potentially devastating, events.

3 Results

This section consists of discussions of the results as they apply to each SOPAC nation included in the study. The diagrams presented in this section have been limited to hazard curves for return periods of between 10 and 2000 years, and maximum amplitude exceedence and regional weighted deaggregated hazard maps at 2000 year return periods. For some nations the results have been further divided, either because of geographic spread, or because different regions have significantly different hazard profiles.

In each section there will be one figure containing three hazard maps for that region. Part (a) shows the hazard curves, (b) the regional weighted deaggregated hazard map and (c) is the maximum amplitude map for the 2000 year return period. For a more detailed explanation of the maps, please see Section 1.3.

The diagrams and discussion in this section can only give an overview of the magnitude and source of the hazard faced by each nation. The maximum amplitude maps are restricted to a 2000 year return period, and the regional weighted deaggregated hazard maps only give a general idea of the source of the hazard for the region as a whole. The KML files on the accompanying DVD can be used to gain a more detailed picture of the hazard of each nation. For example, if one is interested in the source of the hazard at a particular location one should look on the accompanying DVD for a deaggregated hazard map drawn for a model output point close to that location.

In each section, we also briefly mention whether there were any recorded effects of the 1960 Chile tsunami on the country. This information should be only taken as a guide to the possible effects of large tsunami on that nation. The details of the inundation depend critically on the direction and earthquake source properties and can vary from tsunami to tsunami. The amount of information on the effects of the 1960 Chile tsunami is also biased towards locations where we have extant records of the impact of the tsunami. Some islands may be more severely impacted by this event in specific areas, but the sources we consulted may not have included that information. For a summary of all the information concerning the 1960 tsunami, see Appendix C.

3.1 American Samoa

The hazard profile of American Samoa separates neatly between Swain's Atoll and the main islands of Tutuila, Aunuu, Ofu, Olosega and Tau. Figure 6(a) shows that maximum amplitudes (in 100 metres of water) for a 100 year return period are approximately 20 centimetres at Swain's Atoll and 30 to 40 centimetres near the main islands, rising for a 2000 year return period to around 90 centimetres and 2.2 metres respectively (see also Figure 6(c)). Figure 6(b) shows that the hazard at the 2000 year return period is dominated by the Tonga trench, as is to be expected given its proximity.

The tsunami generated by the 1960 Chile earthquake reached a maximum run-up height of over three metres at Pago Pago village on Tutuila island (Allport and Blong, 1995). Buildings were moved off their foundations and a house washed into the bay. No loss of life was reported. Note that the most of the 1 in 2000 year hazard to American Samoa comes from sources to the west of the islands. Therefore any tsunami from those sources may affect American Samoa quite different to the 1960 tsunami.

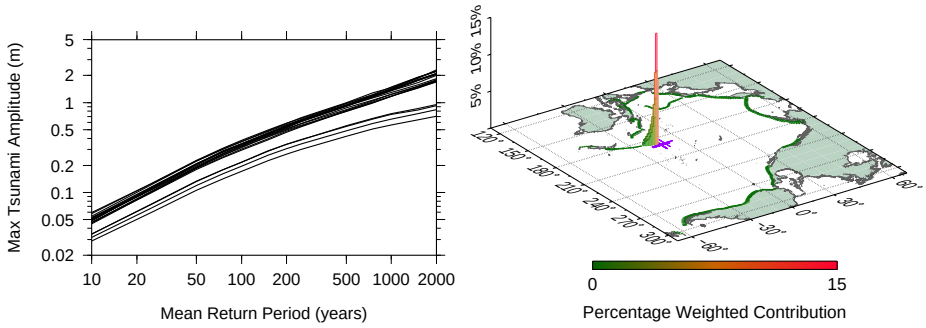

(a) (b)

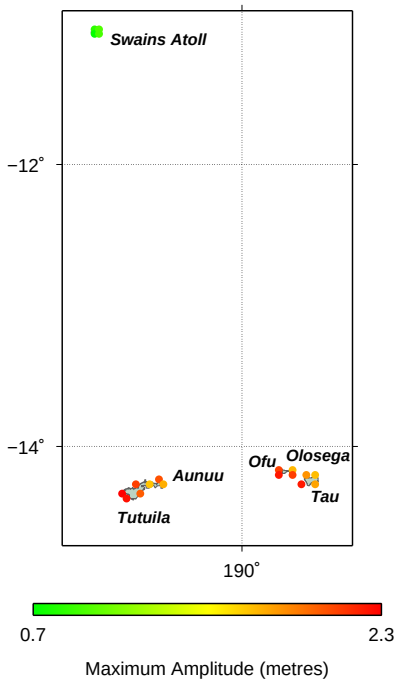

(c)

Figure 6: American Samoa:- (a) Hazard curves for all model output points. (b) Regional weighted deaggregated hazard. (c) Maximum amplitude at a 2000 year return period for all model output points.

3.2 The Cook Islands

The hazard at the 2000 year return period for the northern Cook Islands (latitude greater than -15°) is lower than that for the southern islands. This is clearly the result of the location and orientation of the most significant source of tsunamegenic earthquakes for this nation, the Tonga trench, which extends northwards only to about -15°, and which is oriented so as to direct most tsunami energy south of the northern group of islands (Figure 5). The 2000 year maximum amplitudes are of the order of 1.7 metres for the northern islands and up to 2.8 metres in parts of the southern group (Figure 7(c)), while the 100 year maximum amplitudes range from about 0.3 to 0.4 metres (Figure 7(a)). At the 2000 year amplitude level the hazard is dominated by the Tonga trench (Figure7(b)).

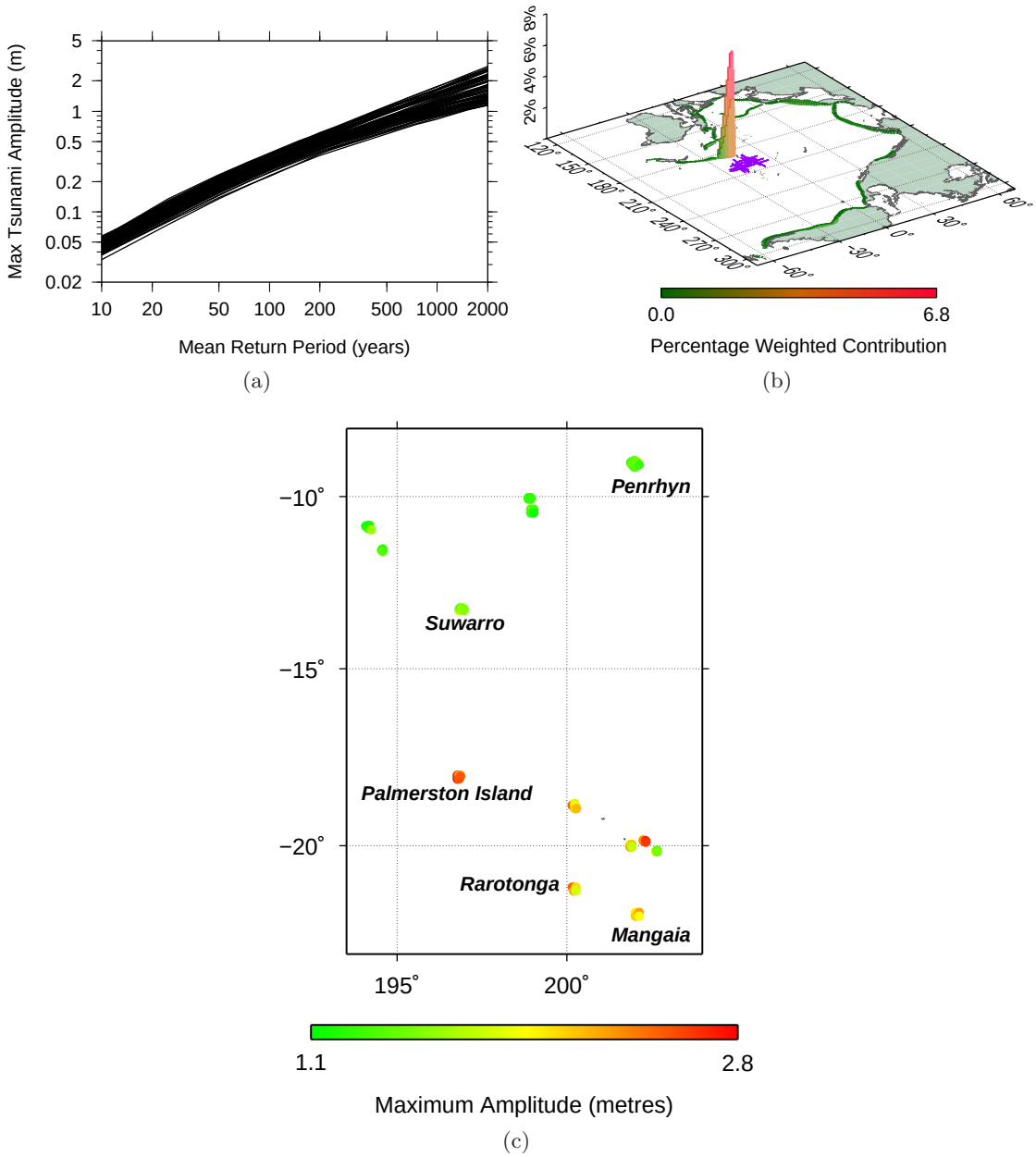

Figure 7: Cook Islands:- (a) Hazard curves for all model output points. (b) Regional weighted deaggregated hazard. (c) Maximum amplitude at a 2000 year return period for all model output points.

3.3 Fiji

As Figure 8(b) shows, the hazard at the 2000 year return period is dominated by the Tonga trench, with some contribution from the New Hebrides trench. This is reflected in the maximum amplitudes at the 2000 year return period (Figure 8(c)), which range from 1 to 3.3 metres with the amplitudes in the eastern islands and on the eastern coast of Vanua Levu being significantly higher than elsewhere. For a return period of 100 years the maximum amplitudes range from 0.2 to 0.6 metres. In Fiji reports of the 1960 tsunami appear to be confined to the effects in Suva harbour. The maximum runup was reported to be about 0.5 metres, and the tsunami induced a powerful surge in the harbour. Many boats sustained damage, but no loss of life was recorded (Allport and Blong, 1995). As with American Samoa, the direction of this wave is quite different from the zones that contribute the most to the 1 in 2000 year tsunami hazard.

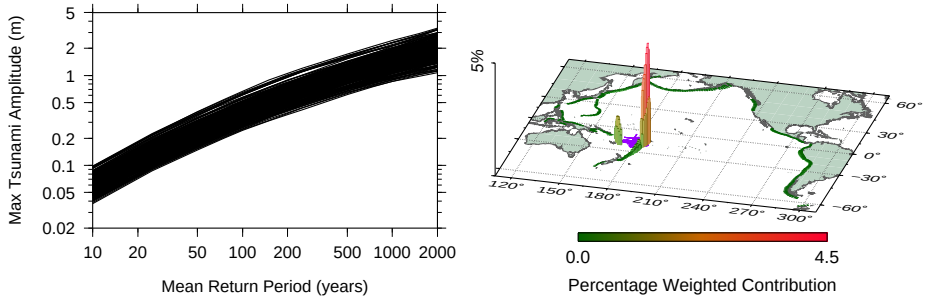

(a) (b)

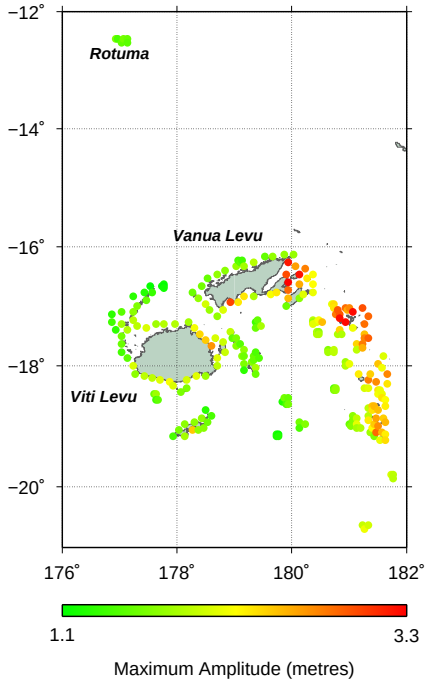

(c)

Figure 8: Fiji:- (a) Hazard curves for all model output points. (b) Regional weighted deaggregated hazard. (c) Maximum amplitude at a 2000 year return period for all model output points.

3.4 French Polynesia

3.4.1 French Polynesia: The Society Islands

The major contribution to the hazard of the Society Islands (2000 year return period) comes from the Tonga trench (Figure 9(b)). Some hazard also comes from the Peru, Chile and Kurils subduction zones. The major islands can expect maximum amplitudes at the 2000 year return period of around 2 metres (Figure 9(c)). The maximum amplitudes at a 100 year return period are much smaller, of the order of 0.2 to 0.5 metres (Figure 9(a)).

In French Polynesia many of the islands are protected by outer reefs and deep lagoons from the effects of the 1960 tsunami, with rather steep bathymetry offshore, and in most cases only slight damage was sustained. No loss of life was recorded throughout the islands. The average runup surveyed in Tahiti was 1.7 metres. Larger runups, up to 3.4 metres, were recorded along the north shore of the island which is more exposed to the open ocean (Vitousek, 1963).

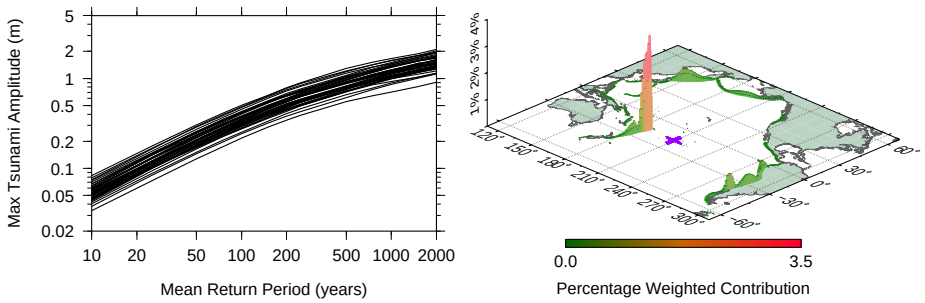

(a) (b)

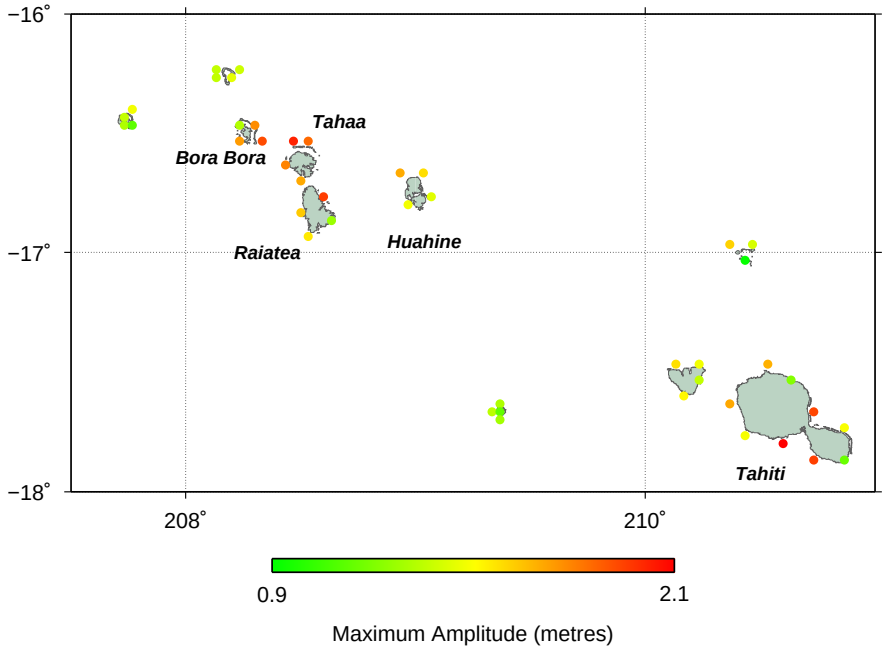

(c)

Figure 9: French Polynesia: Society Islands:- (a) Hazard curves for all model output points. (b) Regional weighted deaggregated hazard. (c) Maximum amplitude at a 2000 year return period for all model output points.

3.4.2 French Polynesia: The Marquesas Islands

The large 2000 year maximum amplitude ($\approx$ 3.8 metres) computed at one model output point on Hiva Oa (Figure 10(c) and the uppermost curve in Figure 10(a)) should be interpreted with caution; it may be a real effect or it may be an artefact of the complex bathymetry in the region. A more detailed study of this part of the coast would be required to clarify this. Regardless of this, Figure 10(c) indicates 2000 year amplitudes of about 2.6 metres off Nuku Hiva and at least 2.8 metres off Hiva Oa. At a return period of 100 years the maximum amplitudes over the region vary from around 0.3 to 0.7 metres. The major contributors to the hazard for this region at a 2000 year return period are the northern part of the Chile trench, and the southern part of the Peru trench (Figure 10(b)).

The greatest effects in French Polynesia from the 1960 tsunami were felt in the Marquesas Islands which have few outer reefs and more gradual changes in offshore bathymetry. Runups of at least 4.5 metres (possibly up to nine metres) were observed. Destruction of buildings near the shore was reported (Vitousek, 1963).

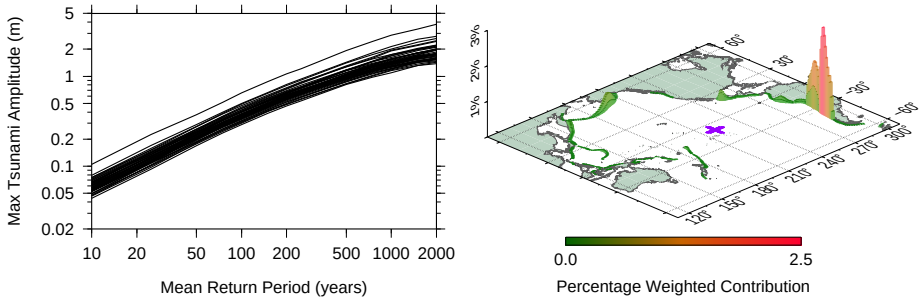

(a) (b)

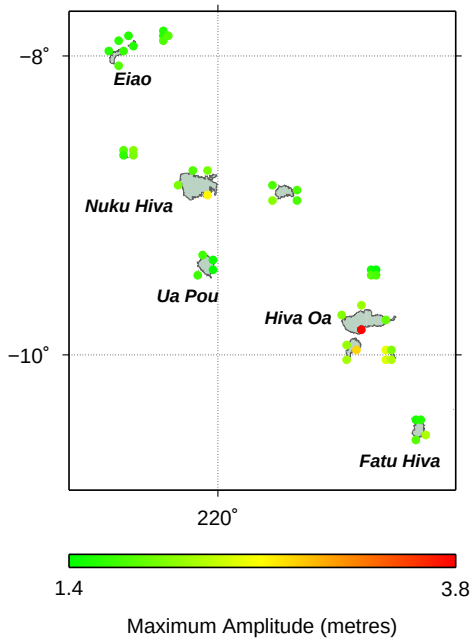

(c)

Figure 10: French Polynesia: Marquesas Islands:- (a) Hazard curves for all model output points. (b) Regional weighted deaggregated hazard. (c) Maximum amplitude at a 2000 year return period for all model output points.

3.4.3 French Polynesia: The Acteon Group, Gambier Islands and southeast Tuamotu Archipelago

Maximum amplitudes at a 2000 year return period of up to 2.3 metres were computed near Mururoa, 2.5 metres near the Acteon Group, 2.2 metres near Marutea and 2.0 metres near the Gambier Islands (Figure 11(c)). For a return period of 100 years the maximum amplitudes ranged from about 0.3 to 0.5 metres over the region as a whole. The major source of hazard for the region at a 2000 year return period was the Tonga trench, with significant contributions from the Kermadec, Peru and Chile trenches (Figure 11(b)).

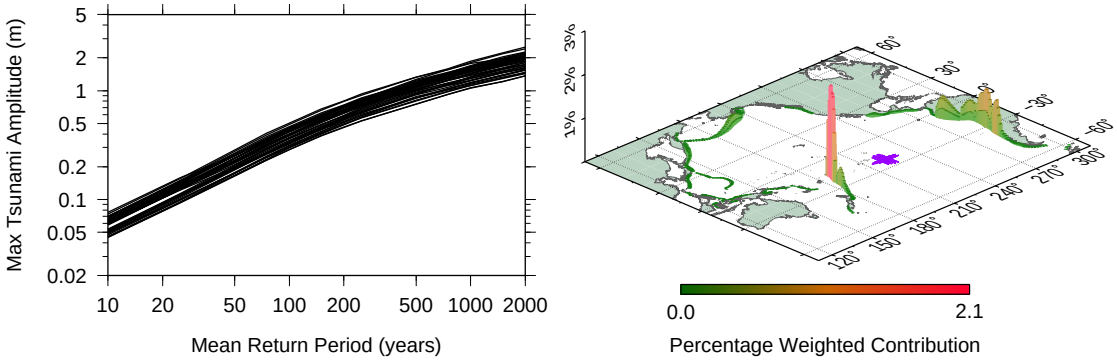

(a) (b)

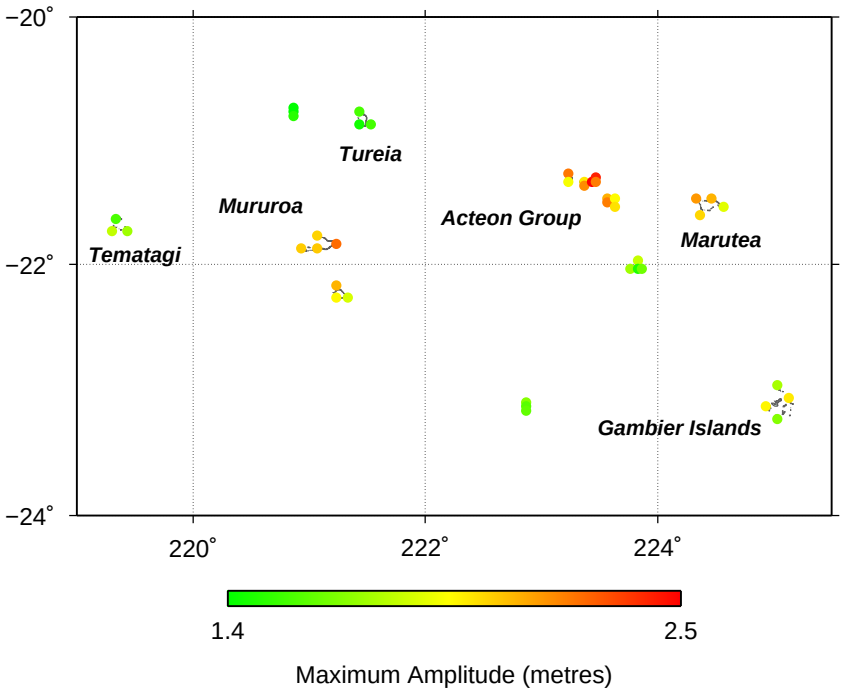

(c)

Figure 11: French Polynesia: The Acteon Group, Gambier Islands and southeast Tuamotu Archipelago:- (a) Hazard curves for all model output points. (b) Regional weighted deaggregated hazard. (c) Maximum amplitude at a 2000 year return period for all model output points.

3.4.4 French Polynesia: The Austral Islands

The 2000 year maximum amplitudes are uniformly of the order of 1.5 to 2 metres across the Austral Islands at a 2000 year return period, and 0.3 to 0.4 metres at a 100 year return period (Figure 12(a)). The dominant source of hazard for the region is the Tonga trench (Figure 12(b)).

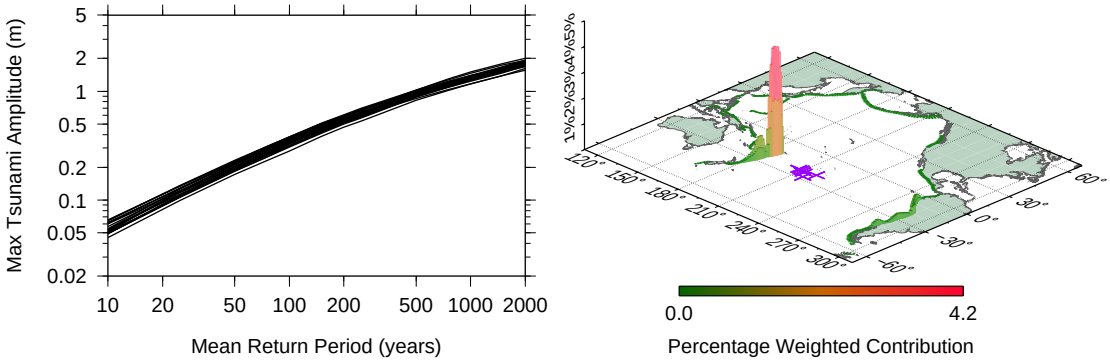

(a) (b)

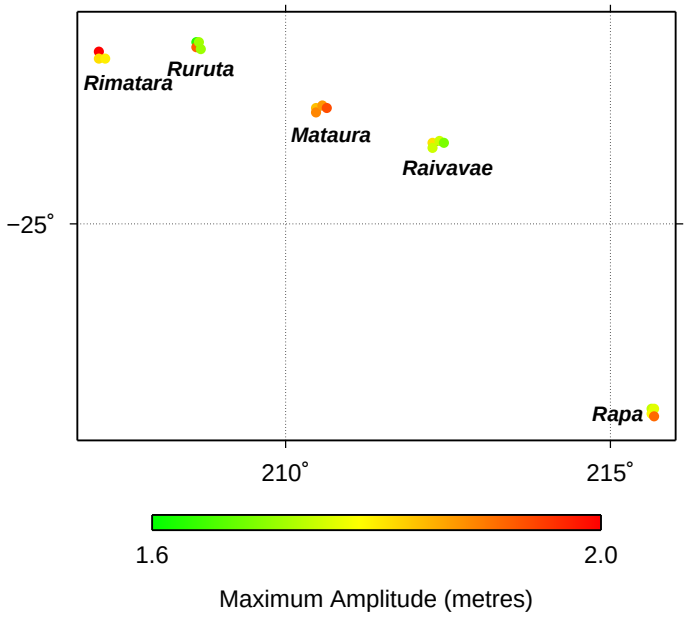

(c)

Figure 12: French Polynesia: The Austral Islands:- (a) Hazard curves for all model output points. (b) Regional weighted deaggregated hazard. (c) Maximum amplitude at a 2000 year return period for all model output points.

3.4.5 French Polynesia: The Tuamotu Archipelago

Maximum amplitudes of the order of 2 to 3 metres were computed in the northeastern and southwestern parts of the archipelago, particularly around Kaukura and Reao (Figure 13(c)). For a return period of 100 years maximum amplitudes of 0.5 to 0.6 metres can be expected throughout much of the archipelago. The hazard for the region at a 2000 year return period originates from the Tonga, Peru and Chile trenches(Figure 13(b)).

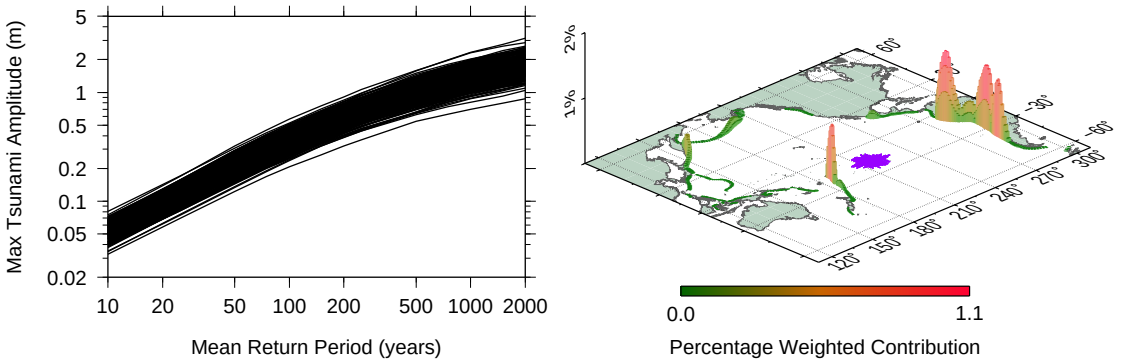

(a) (b)

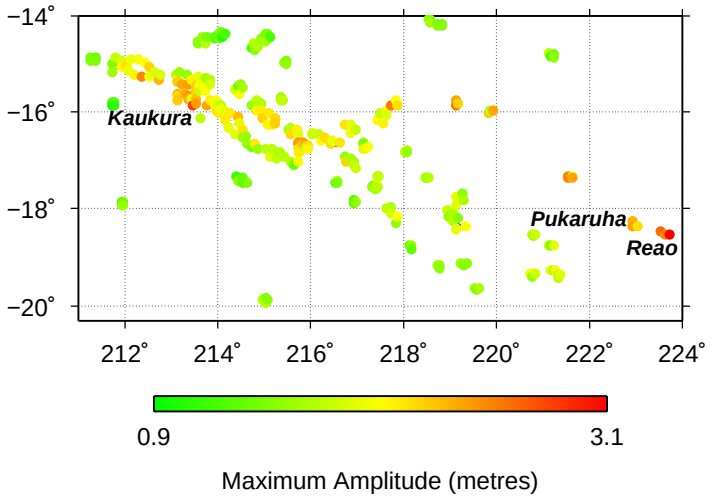

(c)

Figure 13: French Polynesia: The Tuamotu Archipelago:- (a) Hazard curves for all model output points. (b) Regional weighted deaggregated hazard. (c) Maximum amplitude at a 2000 year return period for all model output points.

3.5 Guam

The Mariana trench lies close to Guam, to the south and east, and the highest amplitudes for a 2000 year return period, up to 4.9 metres, are expected off the southern and eastern coasts (Figure 14(c)). For a 100 year return period the maximum amplitudes are of the order of 0.5 to 0.6 metres for all model output points (Figure 14(a)). Figure 14(b) shows that in addition to the Mariana trench, the Philippines Trench is also a significant source of hazard at a 2000 year return period.

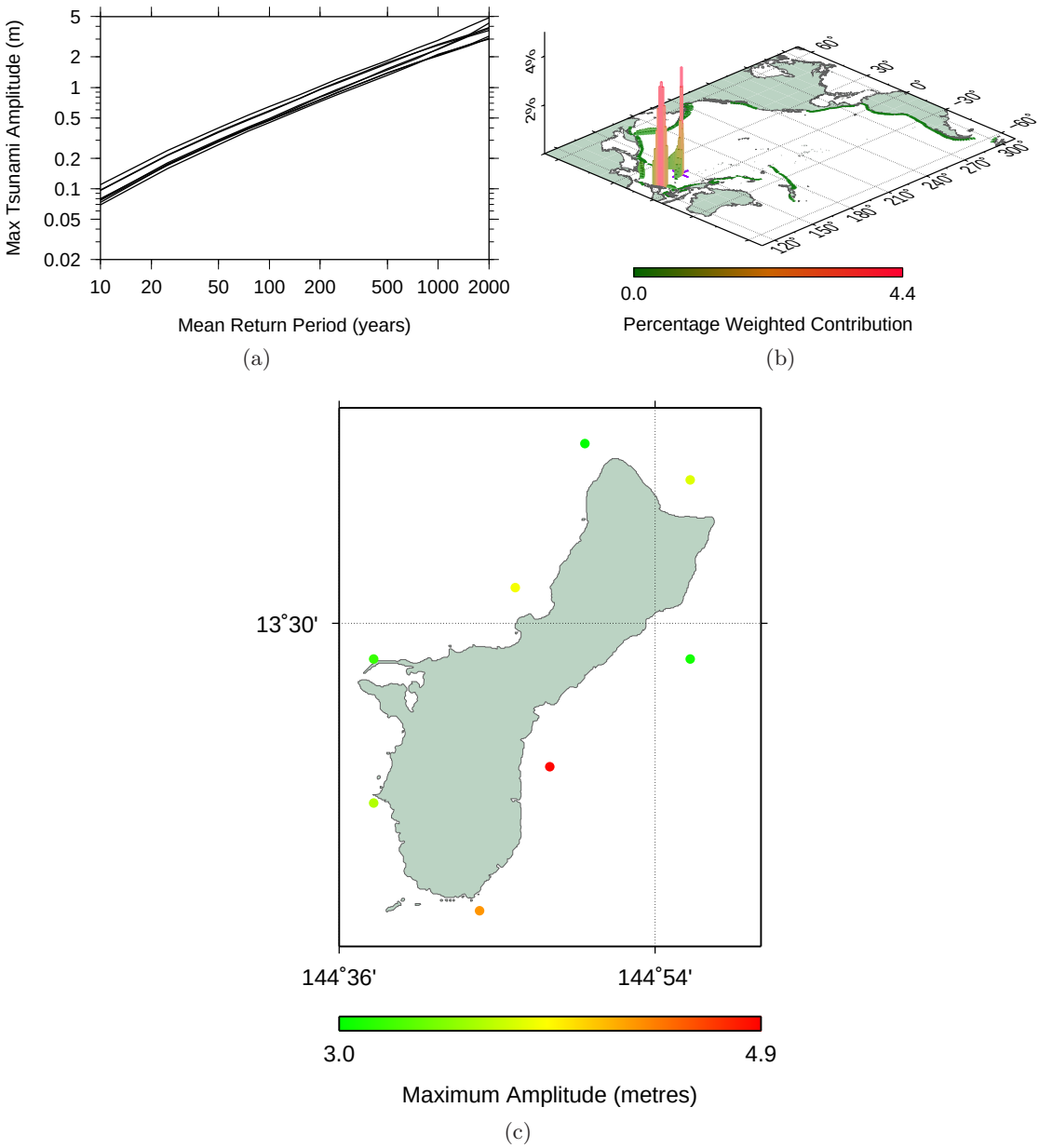

Figure 14: Guam:- (a) Hazard curves for all model output points. (b) Regional weighted deaggregated hazard. (c) Maximum amplitude at a 2000 year return period for all model output points.

3.6 Kiribati

3.6.1 Kiribati: The Gilbert Islands

Over much of the of the Gilbert Islands maximum amplitudes for a 2000 year return period were computed to be of the order of 1.0 to 1.4 metres, with generally lower amplitudes in the most southerly islands (Figure 15(c)). At a return period of 100 years maximum amplitudes of the order of 0.3 to 0.4 metres were typical. Figure 15(b) shows most of the hazard originating in the Kurils and New Hebrides trenches, with smaller contributions from the Mariana, Aleutians, Peru, Chile and Tonga trenches.

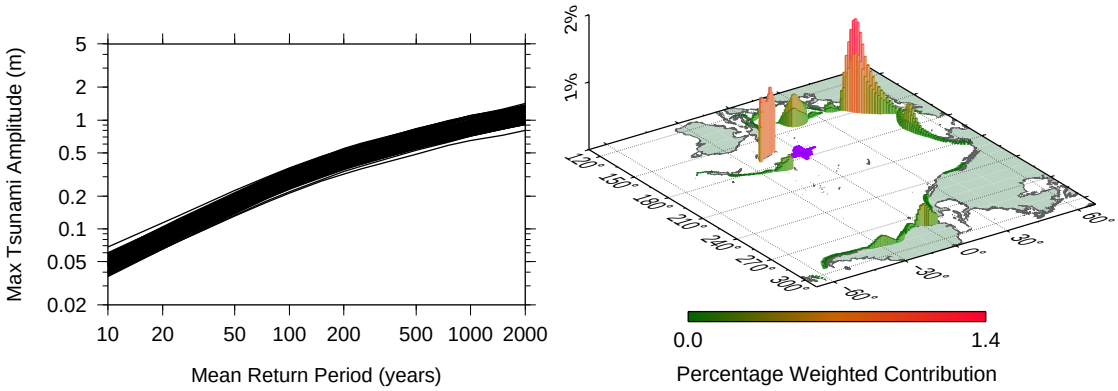

(a) (b)

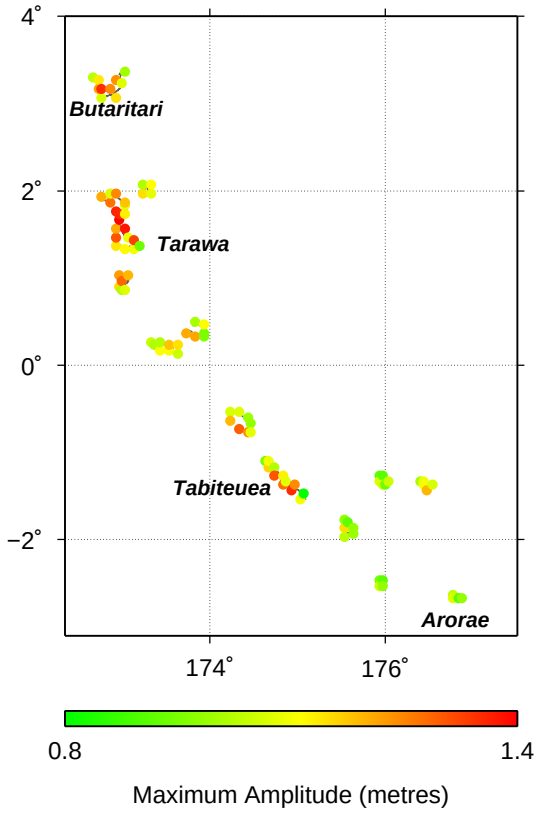

(c)

Figure 15: Kiribati: Gilbert Islands:- (a) Hazard curves for all model output points. (b) Regional weighted deaggregated hazard. (c) Maximum amplitude at a 2000 year return period for all model output points.

3.6.2 Kiribati: The Phoenix Islands

Figure 16(a) shows that the maximum amplitudes at all return periods from 10 to 2000 years are quite uniform over the model output points in the Phoenix Islands, with a maximum amplitude of the order of one metre for a 2000 year return period, and 0.2 to 0.3 metres for a 100 year return period. The origin of the hazard at a 2000 year return period for this region is predominantly the Kurils trench with smaller contributions from the New Hebrides trench, and the Chile trench (Figure 16(b)). Despite its proximity, the Tonga trench contributes little to the hazard because its orientation serves to direct tsunami energy south of the Phoenix Islands.

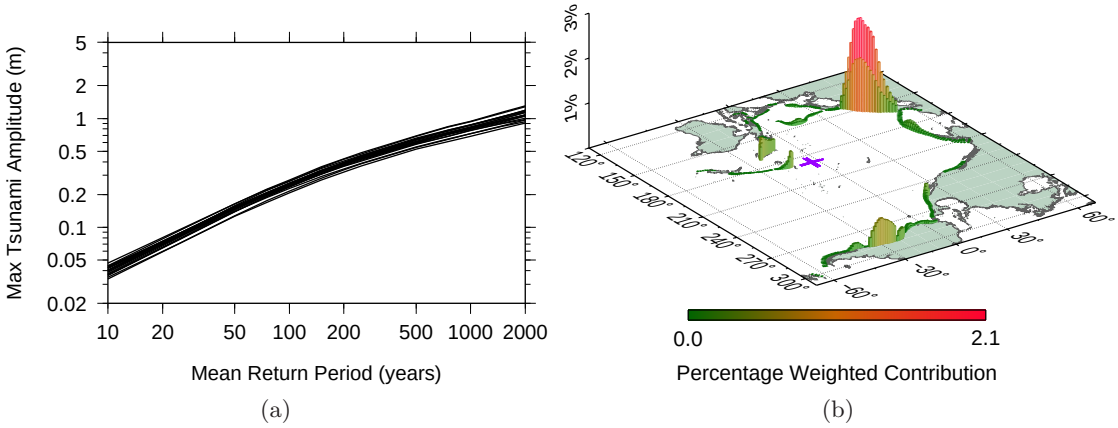

(a) (b)

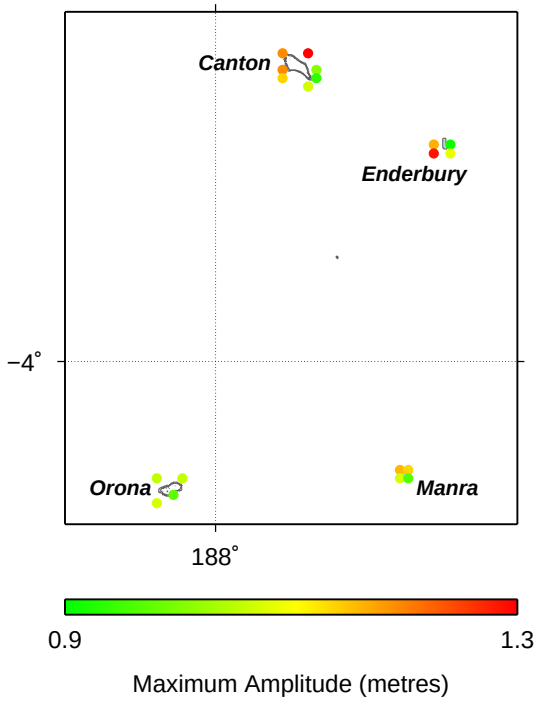

(c)

Figure 16: Kiribati: Phoenix Islands:- (a) Hazard curves for all model output points. (b) Regional weighted deaggregated hazard. (c) Maximum amplitude at a 2000 year return period for all model output points.

3.6.3 Kiribati: The Line Islands

Figure 17(a) shows that the maximum amplitudes are relatively uniform over all model output points in the Line Islands at all return periods between 10 and 2000 years, with a value of around 1.3 to 2.2 metres for a return period of 2000 years, and 0.3 to 0.5 metres for a return period of 100 years. As Figure 17(b) indicates, the major source of hazard for a 2000 year return period for the Line Islands is the Kurils trench, with smaller contributions from the Chile and Peru trenches.

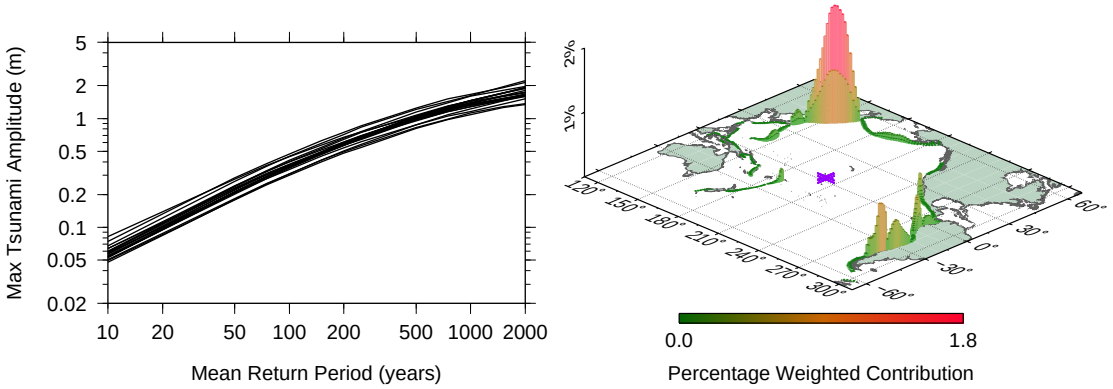

(a) (b)

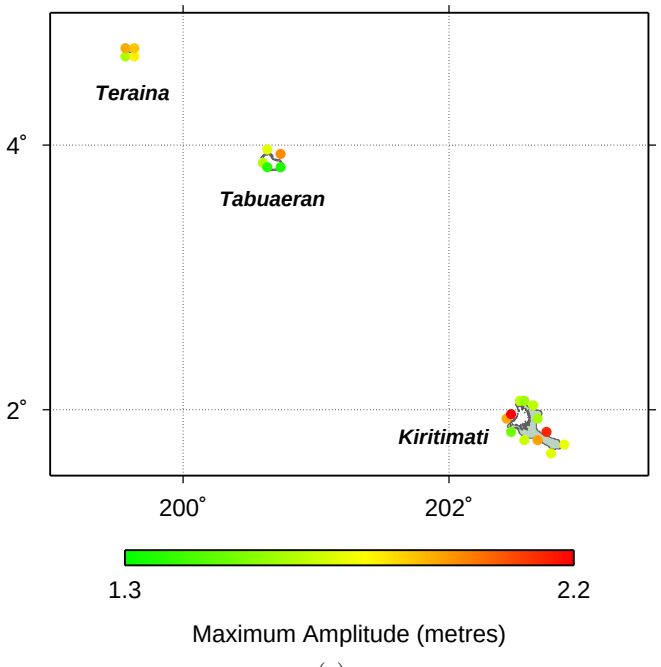

(c)

Figure 17: Kiribati: Line Islands:- (a) Hazard curves for all model output points. (b) Regional weighted deaggregated hazard. (c) Maximum amplitude at a 2000 year return period for all model output points.

3.7 The Marshall Islands

As Figure 18(a) indicates, for a 2000 year return period most of the model output points in the Marshall Islands have a maximum amplitude of between 1 and 2 metres. At a return period of 100 years the maximum amplitudes vary from 0.2 to 0.4 metres. The hazard at a return period of 2000 years is dominated by the Kurils trench, with a smaller contribution from the Mariana trench, and a still smaller one from the Ryukyu trench (Figure 18(b)).

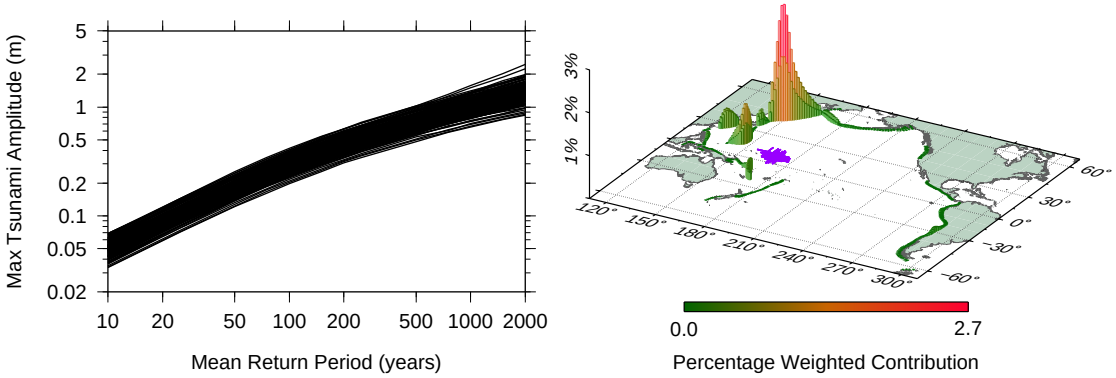

(a) (b)

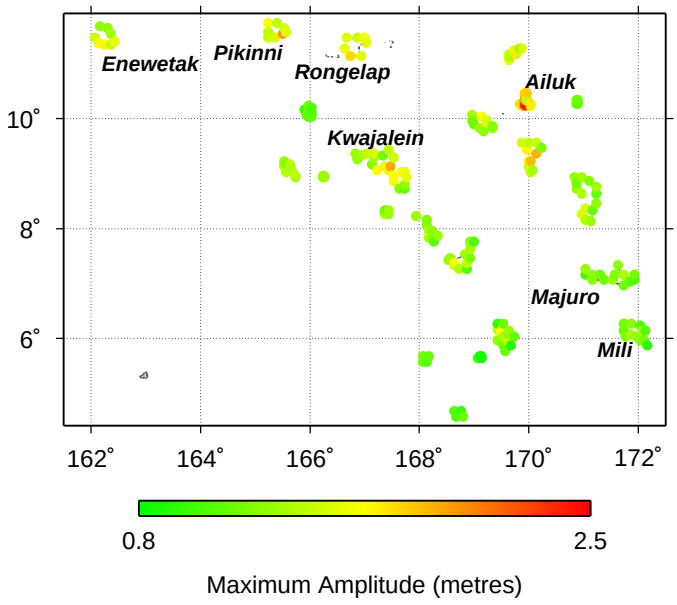

(c)

Figure 18: Marshall Islands:- (a) Hazard curves for all model output points. (b) Regional weighted deaggregated hazard. (c) Maximum amplitude at a 2000 year return period for all model output points.

3.8 The Federated States of Micronesia

The Federated States of Micronesia have a large east - west extent and are best treated in three regions:

1. Yap State
2. Chuuk State
3. Pohnpei and Kosrae

3.8.1 The Federated States of Micronesia: Yap

Figure 19(a) shows that the maximum amplitudes are relatively uniform over all model output points in Yap for return periods of ten to 2000 years, with maximum amplitudes of 1.8 to 2.6 metres expected at the 2000 year return period, and of the order of 0.4 metres at the 100 year return period, with the largest amplitudes being near the island of Yap itself (Figure 19(c)). At the 2000 year return period the deaggregated hazard is spread between the Philippines Trench, the Mariana trench (particularly the southern part) and the New Guinea trench (Figure 19(b)).

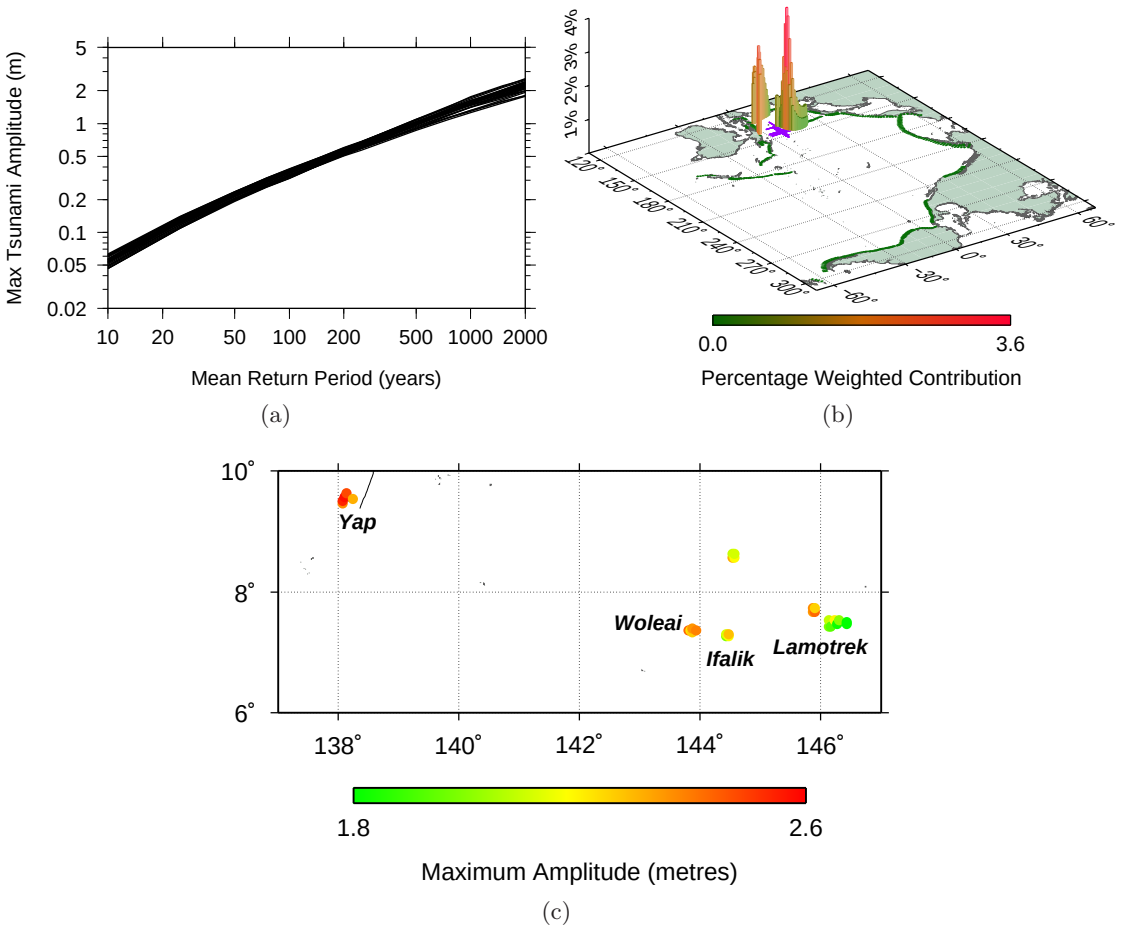

Figure 19: F. S. of Micronesia, Yap State:- (a) Hazard curves for all model output points. (b) Regional weighted deaggregated hazard. (c) Maximum amplitude at a 2000 year return period for all model output points.

3.8.2 The Federated States of Micronesia: Chuuk

The Magur Islands, Hall Islands, Chuuk Islands and Mortlock Islands are coral atolls or lagoons with fringing coral reefs and all have extremely complex bathymetry. Thus one should be cautious in interpreting the maximum amplitude results in these regions, given the resolution of the bathymetry dataset used in the study. This issue is discussed further in Section A.2. Taking a broad view of the results, maximum amplitudes of the order of one to two metres at return periods of 2000 years, and 0.2 metres to 0.5 metres at a 100 year return period can be expected at all of the model output points in the region, (Figures 20(a) and 20(c)). The 2000 year deaggregation (Figure 20(b)) shows that the major contribution to the hazard comes from the Mariana and Philippines trenches, with lesser contributions from the Ryukyu trench, the Kurils trench and the western part of the Aleutians trench.

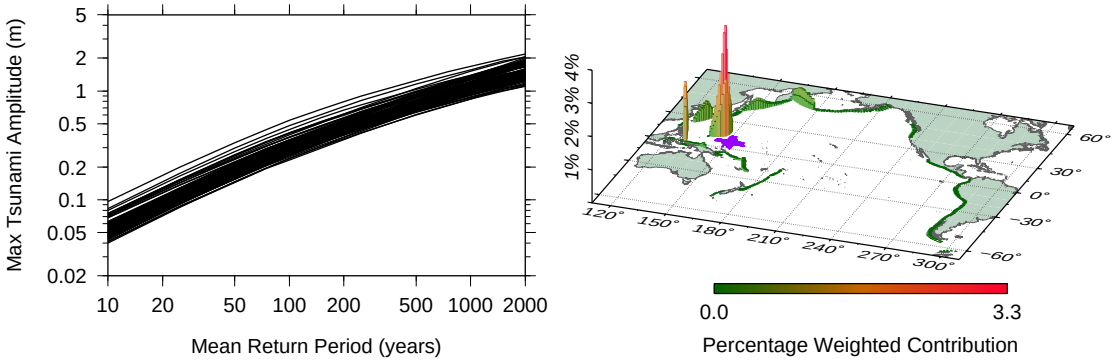

(a) (b)

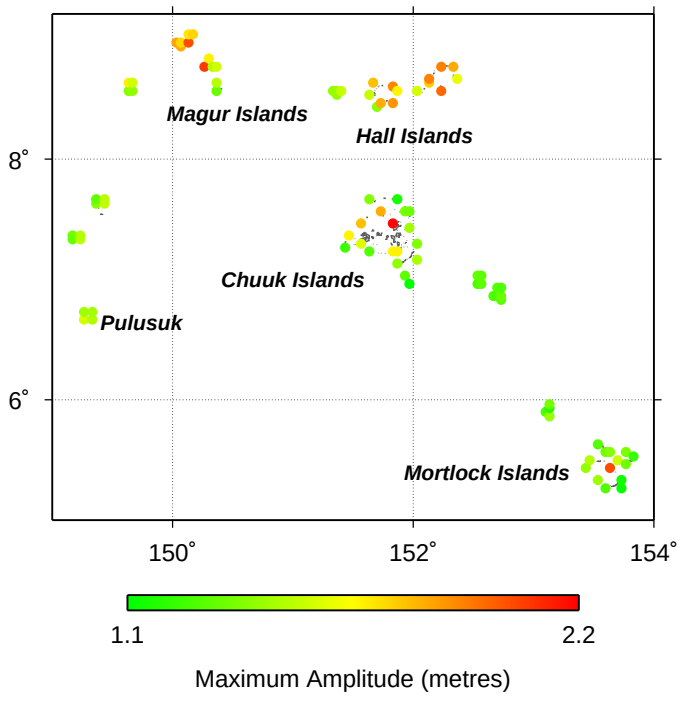

(c)

Figure 20: F. S. of Micronesia, Chuuk State:- (a) Hazard curves for all model output points. (b) Regional weighted deaggregated hazard. (c) Maximum amplitude at a 2000 year return period for all model output points.

3.8.3 Federated States of Micronesia: Pohnpei and Kosrae

Maximum amplitudes for a 2000 year return period vary from 1.1 to 1.9 metres, with the highest values being computed in Oroluk and Pohnpei (Figure 21(c)). At a return period of 100 years the maximum amplitudes vary from around 0.2 to 0.4 metres. Figure 21(b) indicates that, in common with Chuuk, the greatest contribution to the hazard in this region is made by the Mariana and Philippines faults, with significant contributions from the Kurils trench, the Ryukyu and Nankai trenches and to a lesser extent the western part of the Aleutians trench.

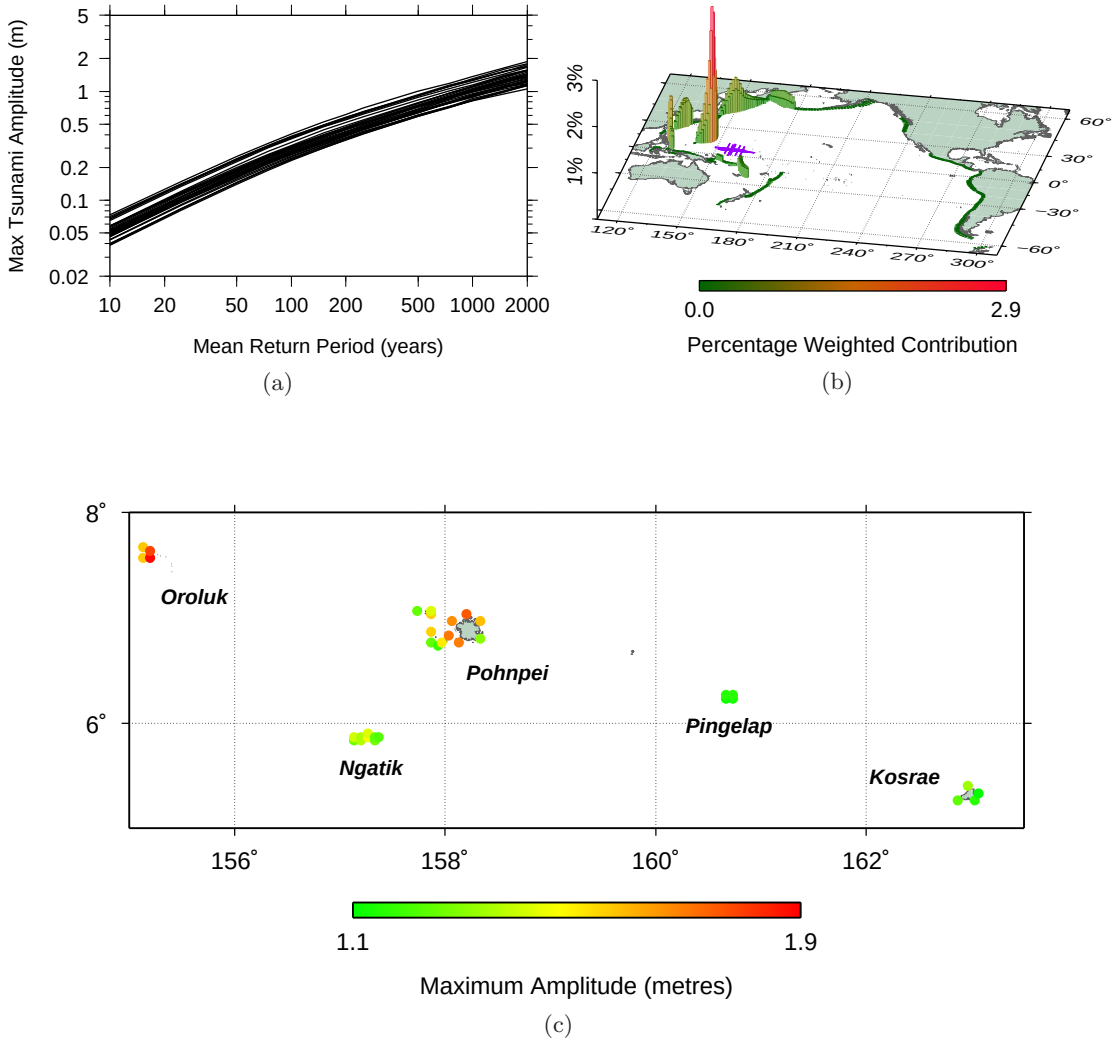

Figure 21: F. S. of Micronesia, Pohnpei and Kosrae:- (a) Hazard curves for all model output points. (b) Regional weighted deaggregated hazard. (c) Maximum amplitude at a 2000 year return period for all model output points.

3.9 Nauru

Nauru has a relatively low hazard, with maximum amplitudes at all model output points computed at about 1 metre for a return period of 2000 years and about 0.2 metres for a return period of 100 years (Figure 22(a)). Figure 22(b) shows that for a 2000 year return period the hazard originates predominantly from the Solomons, New Hebrides and Kurils trenches, with smaller contributions from the Mariana, Philippines and Peru Trenches.

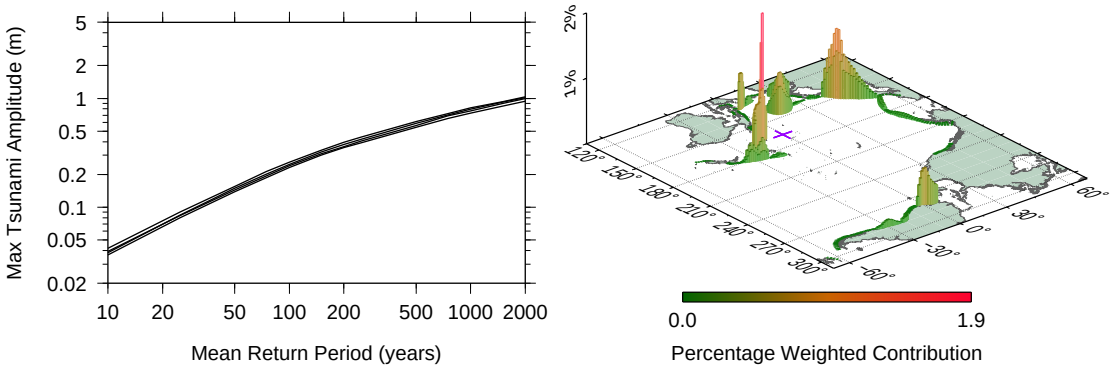

(a) (b)

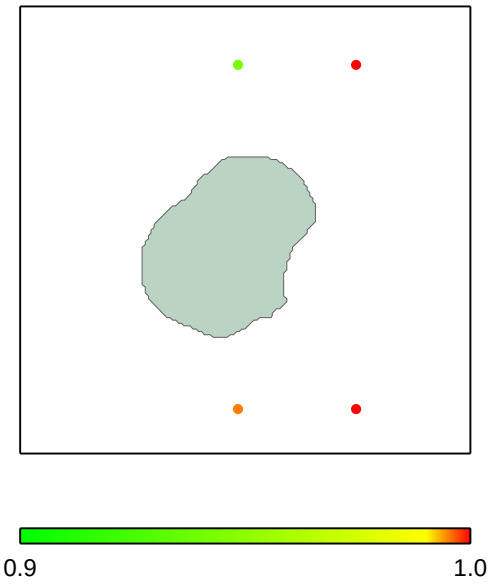

(c)

Figure 22: Nauru:- (a) Hazard curves for all model output points. (b) Regional weighted deaggregated hazard. (c) Maximum amplitude at a 2000 year return period for all model output points.

3.10 New Caledonia

The hazard for New Caledonia originates predominantly from the New Hebrides trench (Figure 23(b)), which lies close to the northeast (the black line in Figure 23(c)). Consequently the maximum amplitudes are somewhat greater on the northeastern coastlines of the islands, with values of up to 4.5 metres, while maximum amplitudes on the southwestern coastlines of Grande Terre are of the order of 1 to 1.5 metres. (Figures 23(a) and 23(c)). For a return period of 100 years the maximum amplitudes range from 0.2 to 0.4 metres, again with the largest amplitudes on the northeastern coastlines.

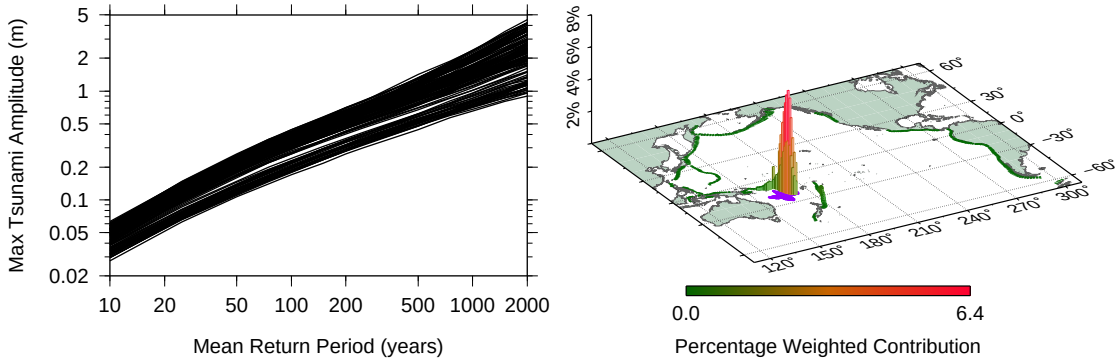

(a) (b)

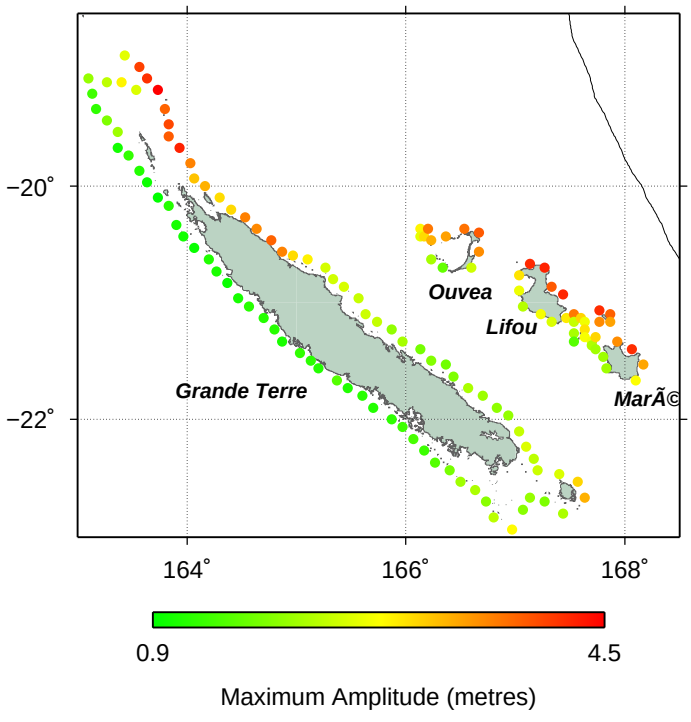

(c)

Figure 23: New Caledonia:- (a) Hazard curves for all model output points. (b) Regional weighted deaggregated hazard. (c) Maximum amplitude at a 2000 year return period for all model output points.

3.11 Niue

The hazard for Niue at a 2000 year return period is from the Tonga trench (Figure 24(b)), which lies just to the west. The maximum amplitudes for a 2000 year return period vary from 2.6 metres for model output points to the east of the island, to a considerable 4.8 metres to the west (Figure 24(c)). At a return period of 100 years the maximum amplitudes are of the order of 0.4 to 0.5 metres at all model ouput points (Figure 24(a)).

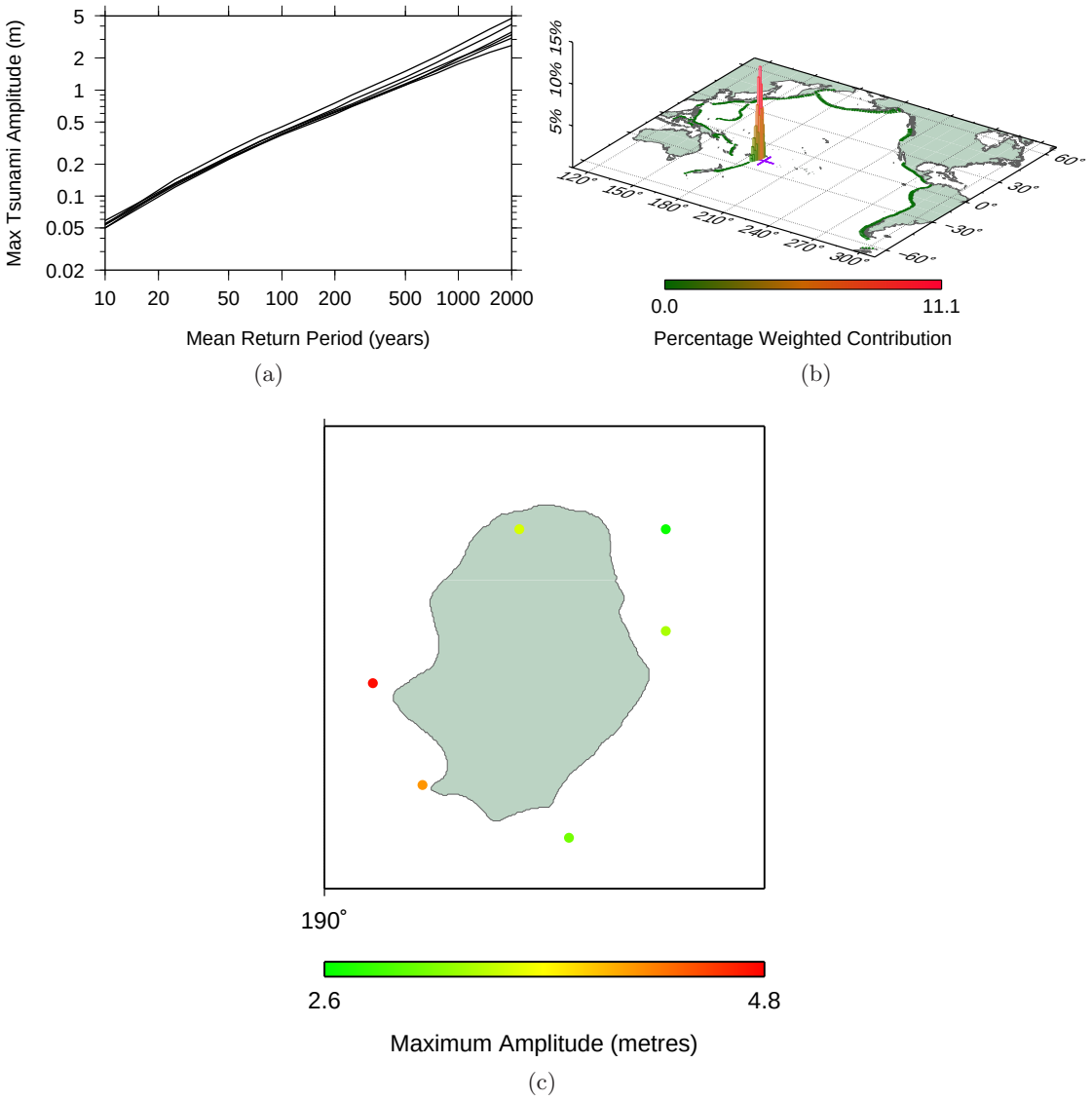

Figure 24: Niue:- (a) Hazard curves for all model output points. (b) Regional weighted deaggregated hazard. (c) Maximum amplitude at a 2000 year return period for all model output points. One point appears to be on dry land because the global bathymetry model is not consistent with the GMT coastline data. The bathymetry data implies that the point is wet, while the coastline data suggests it is on dry land.

3.12 Palau

The maximum amplitudes for a 2000 year return period increase from 2.3 - 2.7 metres near Tobi, Fanna and Sonsorol to 3.5 metres for some model output points on the west coast of Babeldaob and Koror (Figure 25(c)). At a return period of 100 years the maximum amplitudes near Tobi, Fanna and Sonsorol are about 0.3 metres, increasing to 0.5 metres on the western coast of Babeldaob. The hazard at a return period of 2000 years originates almost exclusively from the Philippines trench, which lies just to the west of Palau (Figure 25(b)). There is also a small contribution to the hazard from the New Guinea trench.

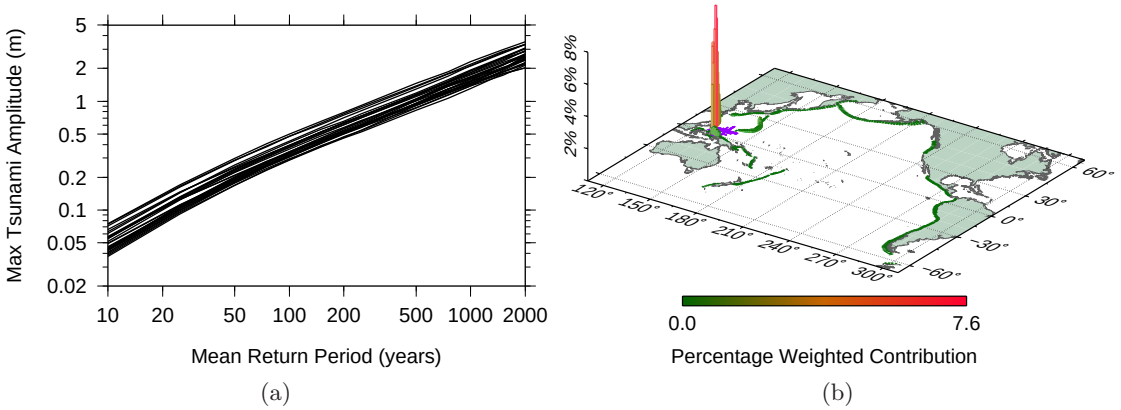

(a) (b)

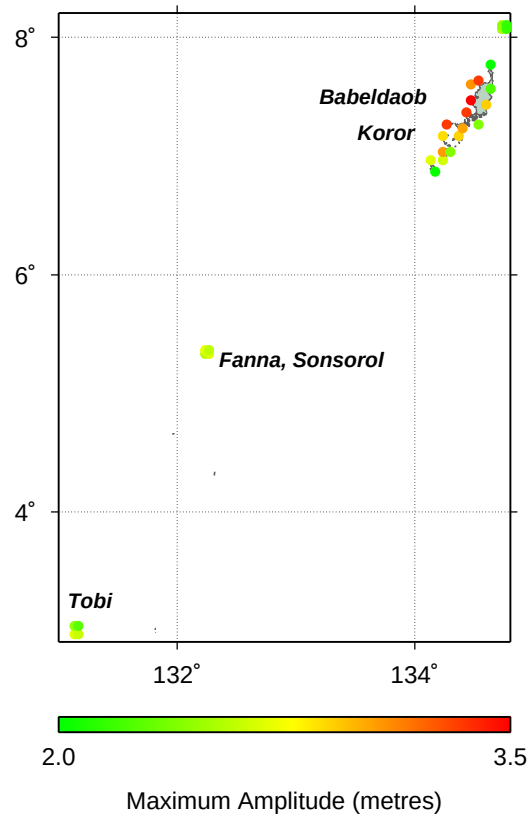

(c)

Figure 25: Palau:- (a) Hazard curves for all model output points. (b) Regional weighted deaggregated hazard. (c) Maximum amplitude at a 2000 year return period for all model output points.

3.13 Papua New Guinea

3.13.1 Papua New Guinea: New Britain, New Ireland and Bougainville

The hazard for this region comes predominantly from the Solomons trench (Figure 26(b)), which lies very close to the south of Bougainville and New Britain and is visible as the black line in Figure 26(c). This is reflected in the amplitudes at a 2000 year return period, with values of up to 3.6 and 3.0 metres on the southern coasts of New Britain and Bougainville respectively (Figure 26(c)). The value of 5.2 metres on the southeast coast of Latangai should be interpreted with caution; it may be an artefact relating to the resolution of the bathymetry used for the computations. There are also significant contributions from the Mariana and Philippines trenches, with lesser contributions from the New Guinea and Kurils trenches. The amplitudes (2000 year return period) on the northern coastlines of these islands are somewhat lower, though still reaching 2.4 metres on New Britain, and 2.0 metres on Latangai and Bougainville. At a 100 year return period amplitudes vary from 0.2 to 0.5 metres throughout the region (Figure 26(a)).

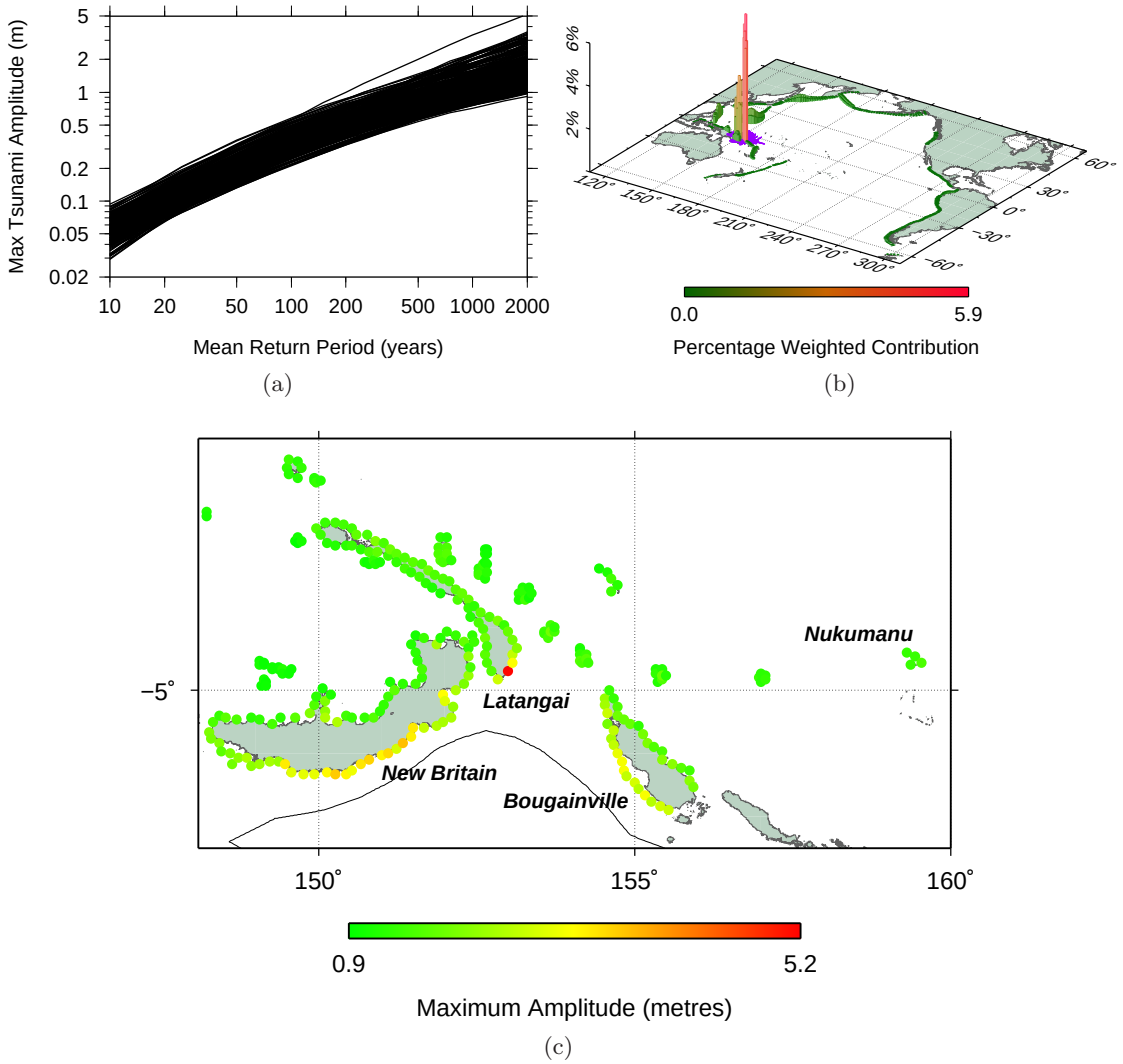

Figure 26: Papua New Guinea: New Britian, New Ireland and Bougainville:- (a) Hazard curves for all model output points. (b) Regional weighted deaggregated hazard. (c) Maximum amplitude at a 2000 year return period for all model output points.

3.13.2 Papua New Guinea: South and West

Referring to Figure 27(c), the largest maximum amplitudes for a 2000 year return period were computed at model output points near Kiriwina and Woodlark (up to 3.9 metres), the northern coast of the Louisiade Archipelago (up to 3.1 metres), and the western part of the northern coastline of the mainland (up to 3.3 metres). The source of the hazard for the region is dominated by the Solomons trench (which affects the areas south of latitude $-6°$, and the New Guinea trench, which affects areas further west and north (Figure 27(b)). Both of these are visible on Figure 27(c). The hazard along the southern coasts of the mainland and the Louisiade Archipelago is lower. At a return period of 100 years, maximum amplitudes of 0.4 to 0.5 metres are expected along the northern coasts of the mainland and the Louisiade Archipelago, and near Kiriwina and Woodlark.

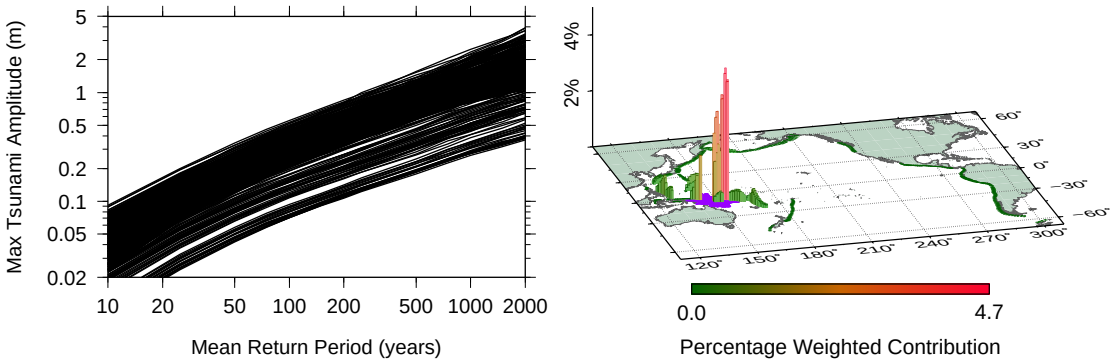

(a) (b)

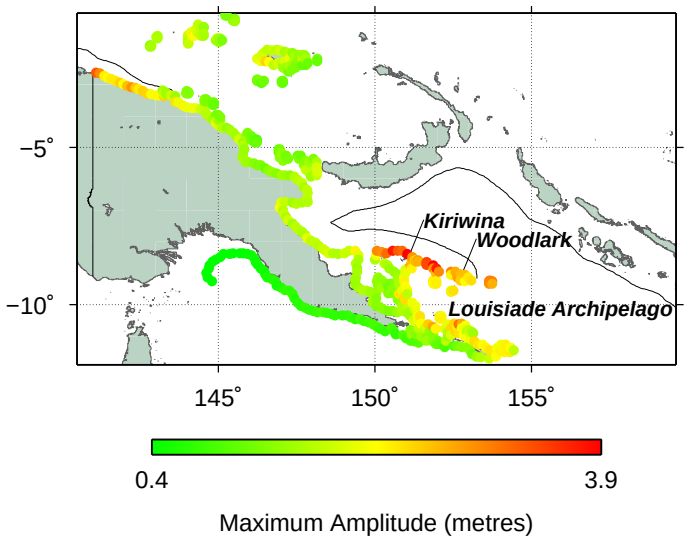

(c)

Figure 27: Papua New Guinea: south and west:- (a) Hazard curves for all model output points. (b) Regional weighted deaggregated hazard. (c) Maximum amplitude at a 2000 year return period for all model output points.

3.14 Samoa

The southern coastlines of Savaii and Upolu have the highest hazard, with maximum amplitudes at a 2000 year return period of the order of 2.3 to 3.4 metres (Figure 28(c)). This is due to the proximity of the Tonga trench, which lies just to the south and is the only significant source of hazard for the region (Figure 28(b)). Maximum amplitudes on the northern coastlines are lower, but still significant, particularly in the case of Upolu (up to 2.0 metres). At a return period of 100 years maximum amplitudes of up to 0.6 metres can be expected on the southern coasts of Savaii and Upolu.

In Western Samoa the tsunami generated by the 1960 Chile earthquake was also most pronounced at Fagaloa Bay (Upolu) where the maximum run-up (the highest point above sea level reached by the wave) was estimated to be about 2.5 metres (Keys, 1963). Minor damage to buildings was sustained and it was reported that the waves carried fuel drums 73 metres inland. Residents, who had been forewarned by announcements on the local radio station, had taken refuge on higher ground and no loss of life occurred. The rest of Western Samoa appears to have escaped undamaged, probably because of screening by offshore reefs, which are absent from Fagaloa Bay (Keys, 1963).

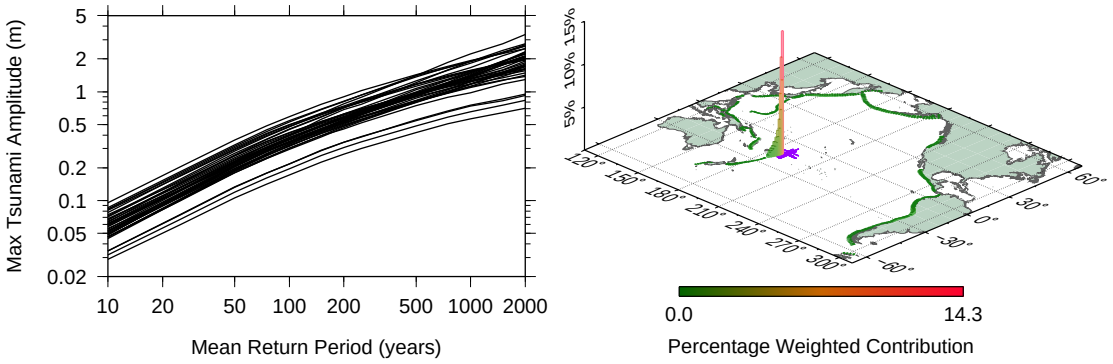

(a) (b)

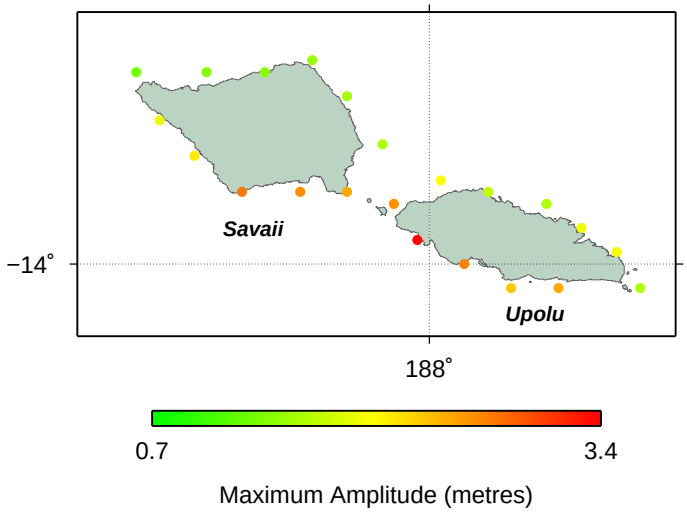

(c)

Figure 28: Samoa:- (a) Hazard curves for all model output points. (b) Regional weighted deaggregated hazard. (c) Maximum amplitude at a 2000 year return period for all model output points.

3.15 The Solomon Islands

The Solomons and New Hebrides trenches are the only significant sources of hazard for this region (Figure 29(b)), with the Solomons trench, which is visible on Figure 29(c), dominating. The southern coastlines of Makira, Guadalcanal and New Georgia, and the northern shore of Rennell have the highest hazard, with maximum amplitudes of around 1.7 to 3.7 metres (Figure 29(c)). At a return period of 100 years maximum amplitudes of 0.2 to 0.5 metres can be expected at all model output points in the region (Figure 29(a)).

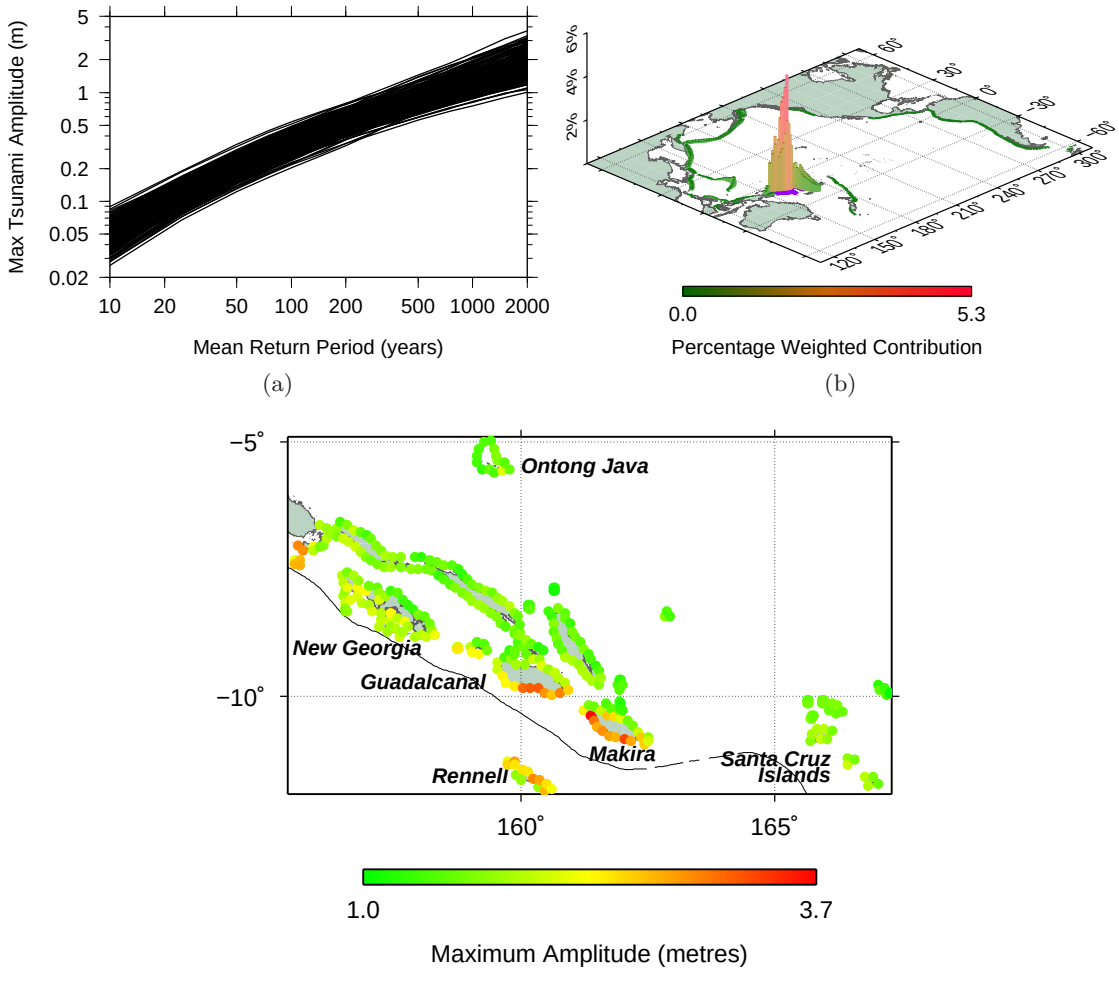

Figure 29: Solomon Islands:- (a) Hazard curves for all model output points. (b) Regional weighted deaggregated hazard. (c) Maximum amplitude at a 2000 year return period for all model output points.

3.16 Tokelau

The hazard is relatively uniform over all model output points in Tokelau, with maximum amplitudes for a 2000 year return period ranging from 1.0 to 1.4 metres, and 0.2 to 0.3 metres at a return period of 100 years (Figures 30(a) and 30(c)). The most significant sources of hazard are the New Hebrides trench and the northern part of the Tonga trench, with smaller contributions from the Kurils trench and the Peru and Chile trenches (Figure 30(b)).

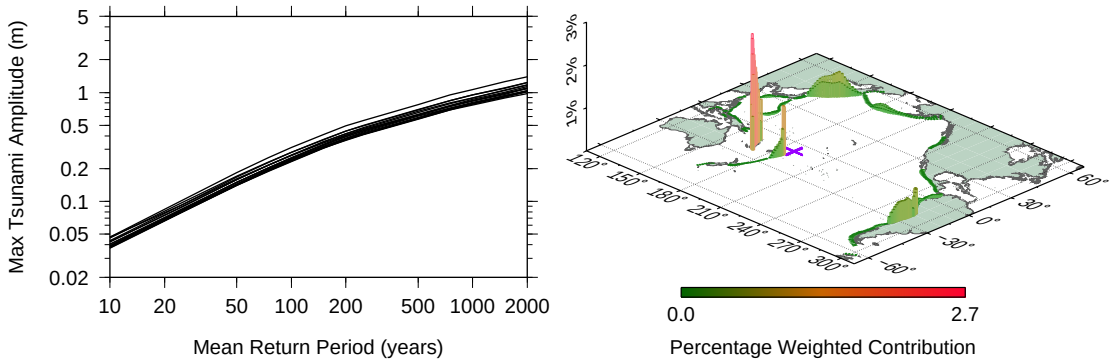

(a) (b)

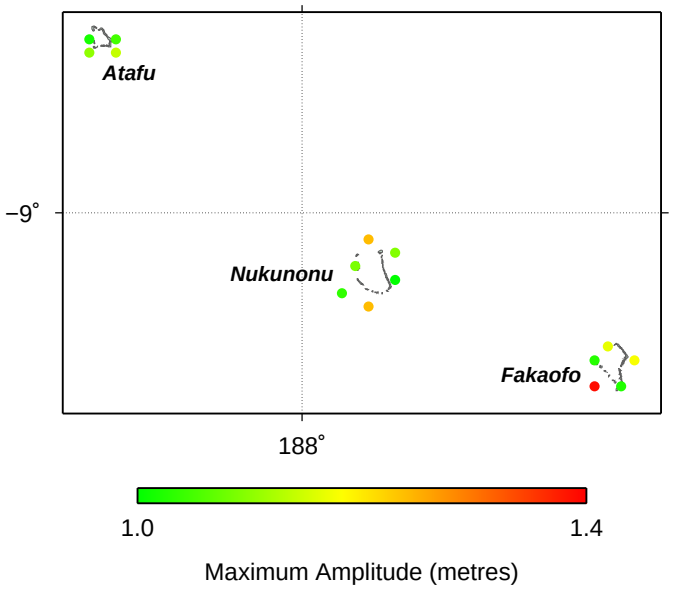

(c)

Figure 30: Tokelau:- (a) Hazard curves for all model output points. (b) Regional weighted deaggregated hazard. (c) Maximum amplitude at a 2000 year return period for all model output points.

3.17 Tonga

Tonga lies just to the west of the Tonga trench, which is the source of hazard for this nation (Figure 31(b)) and part of which is visible in Figure 31(c). At a return period of 2000 years, maximum amplitudes of up to 3.6 metres off Tongatapu, 3.9 metres off Haapai, 4.7 metres off Hunga and 4.3 metres off Niuatoputapu can be expected (Figure 31(c)). In the more westerly islands maximum amplitudes are lower but are still potentially hazardous, for example up to 2.1 metres in Niuafoou. At a return period of 100 years, maximum amplitudes of up to 0.7 metres can be expected in the same regions (Figure31(b)).

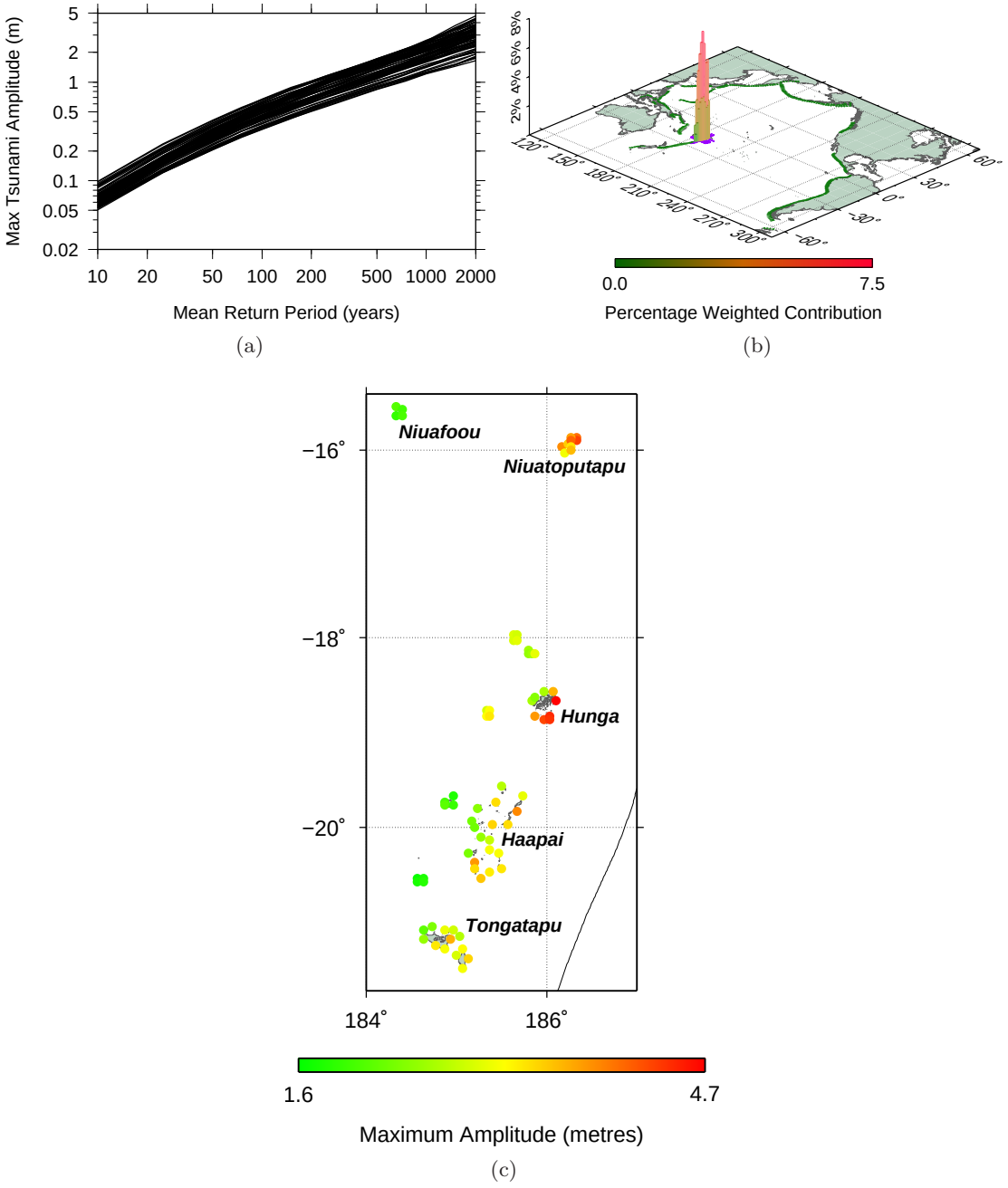

Figure 31: Tonga:- (a) Hazard curves for all model output points. (b) Regional weighted deaggregated hazard. (c) Maximum amplitude at a 2000 year return period for all model output points.

3.18 Tuvalu

The hazard is greater in the southern islands of Tuvalu, with maximum amplitudes (2000 year return period) of up to 1.6 metres in Nukulaelae and around 1.0 to 1.2 metres in Nukufetau and Funafuti (Figure 32(c)). At a return period of 100 years maximum amplitudes of 0.2 to 0.3 metres can be expected at all model output points in the region. The major source of hazard is the New Hebrides trench (Figure 32(b)), which is oriented so as to direct most of the energy from a tsunami originating there toward the southern islands. Some of the hazard at this return period also comes from the Tonga subduction zone.

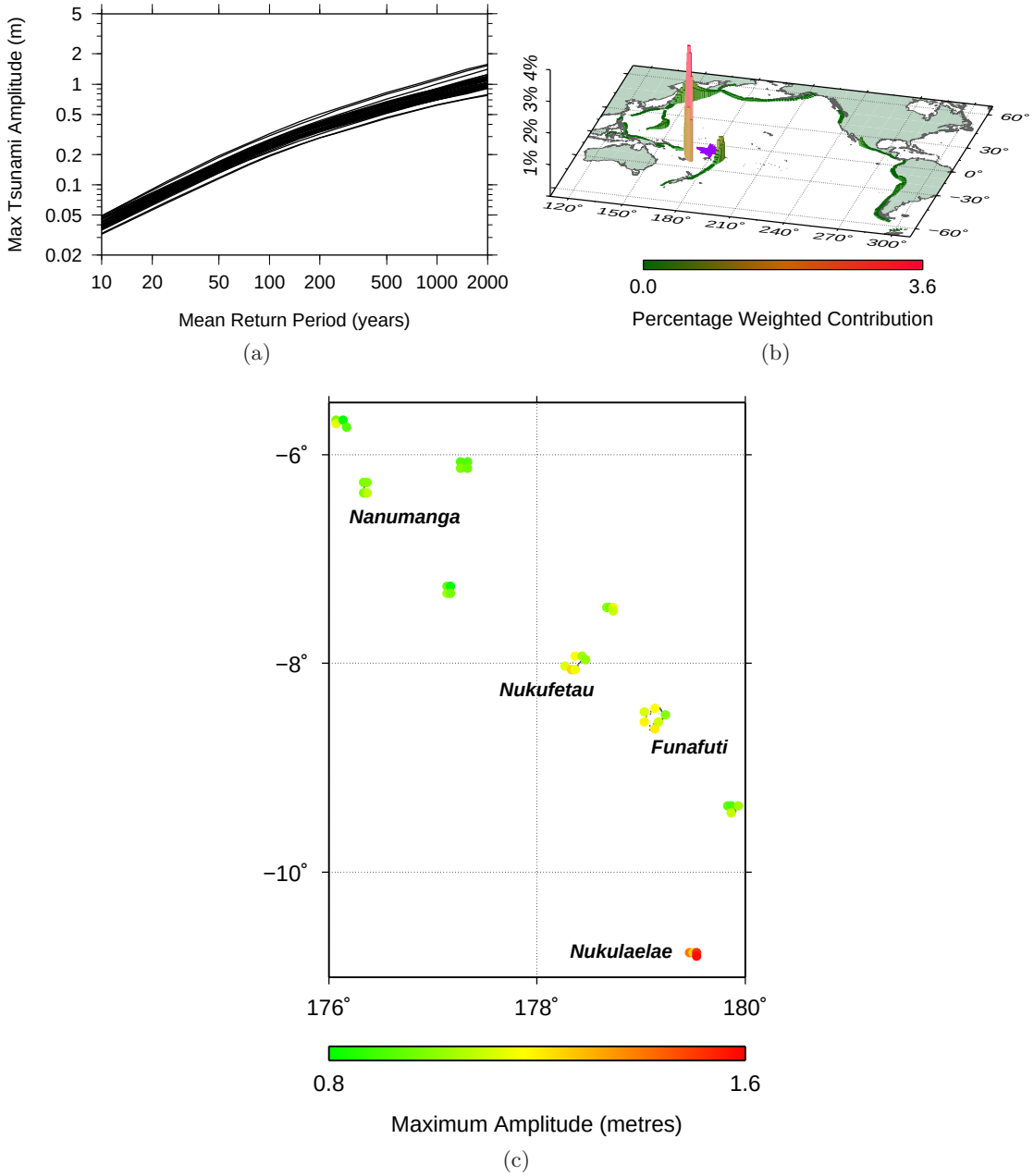

Figure 32: Tuvalu:- (a) Hazard curves for all model output points. (b) Regional weighted deaggregated hazard. (c) Maximum amplitude at a 2000 year return period for all model output points.

3.19 Vanuatu

The New Hebrides trench, visible on Figure 33(c), lies just to the west of Vanuatu and is the primary source of hazard for the region (Figure 33(b)). Maximum amplitudes for a 2000 year return period are significantly higher at model output points on the western shores of the major islands over those on the eastern shores, with values of over 4.0 metres on Espiritu Santo, Malakula, Efate, Erromango, Tanna and Aneityum (Figure 33(c)). Maximum amplitudes at the more easterly islands are lower, though still potentially hazardous; for example they reach 1.9 metres near Pentecost. At a 100 year return period maximum amplitudes of up to 0.6 to 0.7 metres can be expected at some model output points.

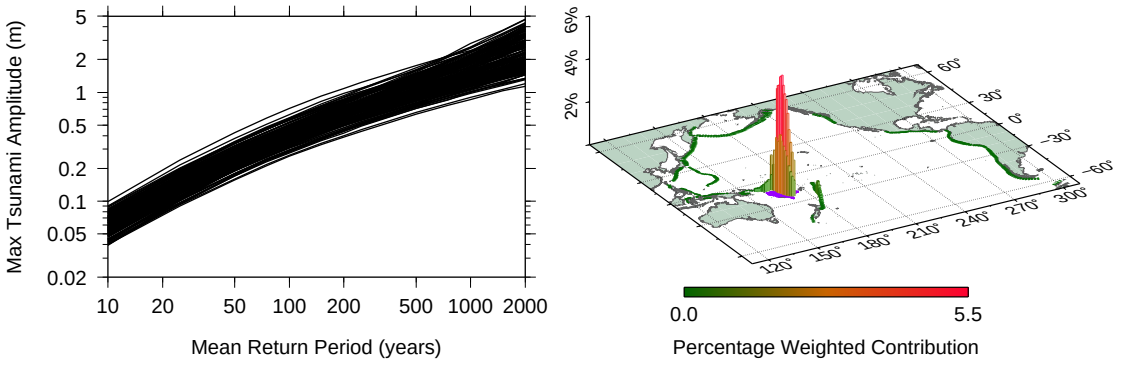

(a) (b)

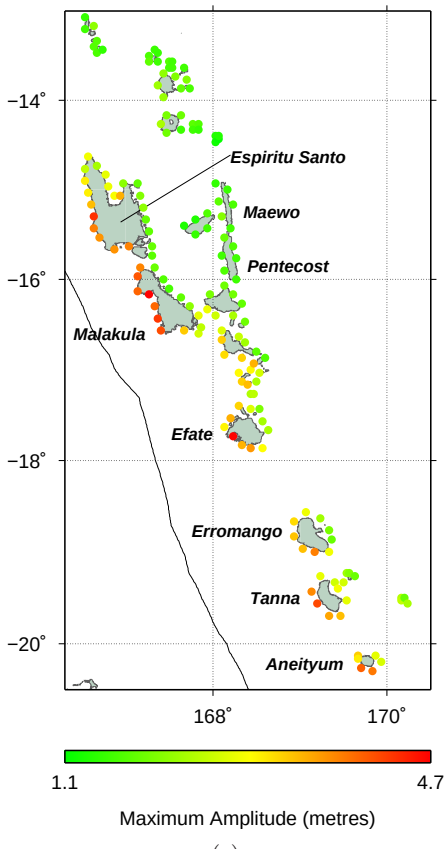

(c)

Figure 33: Vanuatu:- (a) Hazard curves for all model output points. (b) Regional weighted deaggregated hazard. (c) Maximum amplitude at a 2000 year return period for all model output points.

4 Conclusion

In summary, by segmenting the Pacific Rim subduction zones we have modelled nearly 60,000 tsunami to offshore of all the SOPAC nations. The probability of each tsunami was estimated by determining what fraction of the global seismicity would be expected on each zone and partitioning the global seismicity accordingly. For each subduction zone a range of different maximum magnitudes and earthquake source geometry models were included in the final hazard assessment presented here.

This assessment was designed to allow SOPAC to prioritise which nations have the highest tsunami hazard and should be considered for future, more detailed, study. The nations with the highest hazard at the 1 in 2000 year return period level are listed in Table 1 and the hazard curves for the point with the highest hazard in each nation are shown in Figure 34.

Several major conclusions can be drawn from the report:

- Several nations have a very high tsunami hazard. These nations are usually close to a major subduction zone and are perpendicular to it (eg PNG, New Caledonia, Tonga, Guam, Vanuatu). The nearest zone dominates the hazard for these nations, particularly at longer return periods. If a large earthquake occurred at a zone very close to the country, the tsunami may arrive before any warning from any of the global warning centres.
- The SOPAC nations located near the centre of the Pacific have a more moderate hazard, but the sources of the hazard are spread out over a larger number of zones around the Pacific Rim. Potentially dangerous tsunami for these islands can come from a large number of different directions towards the islands.

For more details on specific nations, please see the relevant section in Section 3, the kml files on the accompaning DVD or contact Geoscience Australia directly.

While we believe the overall results of this study are reliable and are useful, we do recommend that more detailed studies be undertaken, particularly of the nations with the highest hazard. In particular, future studies should use a higher resolution and more accurate bathymetry for the southwest Pacific islands. The resolution of the bathymetry used here is not high enough to determine precisely the offshore heights with great confidence, given the complex bathymetry of the region. However, we believe the relative levels of hazard are reliable.

The other major source of uncertainity in this assessment is with our estimate of the liklihood of a major (Mw8+) event for many of the zones. In this assessment, we estimated this liklihood by extrapolating from the frequency of smaller earthquakes. However, we cannot be sure that any given zone can, or ever has, produced an earthquake larger than has been observed for the zone. The only way to reduce this uncertainity is by studies into the palaeo-record of specific islands for evidence of pre-historic large inundations from tsunami. However, given the scale of the problem this is likely to be a slow task.

It is also important to note that high offshore wave heights do not always correspond to high onshore run-ups or large amounts of damage. If the bulk of a island's population is close to sea level then even a moderate to low tsunami may have the potential to cause significant damage. Therefore we recommend more detailed inundation studies of the

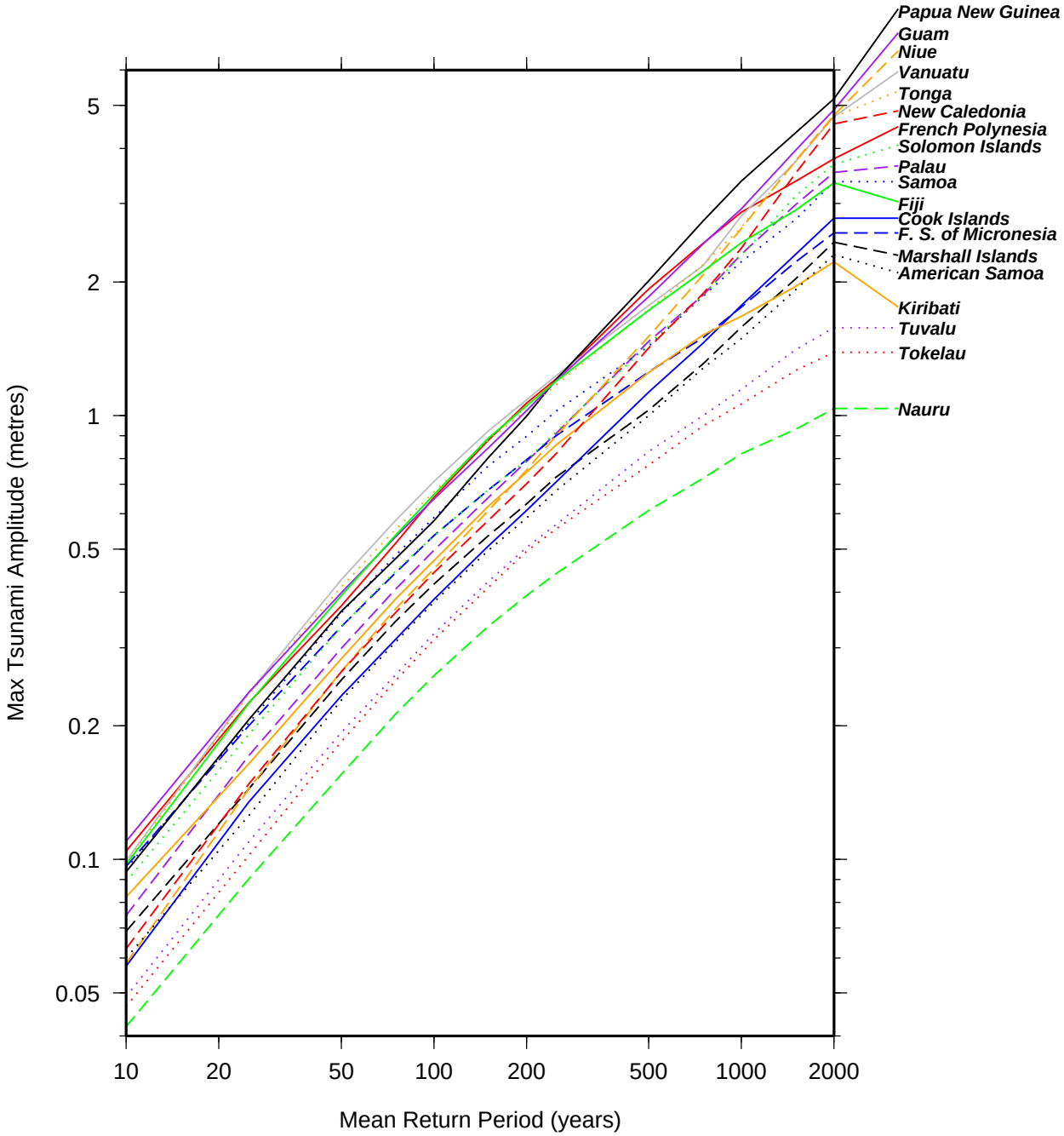

Figure 34: Hazard curves for the nations in the study. For each return period the curve gives the maximum value of the amplitude taken over all the model output points of that nation.

potentially at risk communties be undertaken in order to more confidently quantify the potential impact to the SOPAC nations of a major tsunami reaching the islands.

References

Allport, J.K. and R.J. Blong, 1995. *The Australian Tsunami Database (ATDB)*, Sydney: School of Earth Sciences, Macquarie University.

Barrientos, S.E. and S.N. Ward, 1990. The 1960 Chile earthquake: inversion for slip distribution from surface deformation. *Geophys. J. Int.* **103**, pp.589-598.

Bryant, E., 2001. *Tsunami: the underrated hazard*, Cambridge University Press, Cambridge.

Bassin, C., Laske, G. and G. Masters, 2000. The current limits of resolution for surface wave tomography in North America, *EOS Trans AGU*, **81**, F897. http://mahi.ucsd.edu/Gabi/rem.html.

Bathgate, J., Volti T.. and Greenslade, D. J. M., 2008. The Joint Australian Tsunami Warning Centre: responding to a tsunamigenic earthquake - Puysegur Trench, 30 September 2007. *Preview*, 133, April 2008, pp. 40-44.

Bird, P., 2003. An updated digital model of plate boundaries. *Geochem. Geophys. Geosys.* **4**(3), 1027, doi:10.1029/2001GC000252.

Burbidge, D., Cummins, P. and Mleczko R., 2007. *A Probablistic Tsunami Hazard Assessment for Western Australia: Report to the Fire and Emergency Services Authority of Western Australia*, Geoscience Australia.

Burbidge, D., Mleczko, R., Thomas, C., Cummins, P., Nielsen, O. and T. Dhu, 2008. *A Probabilistic Tsunami Hazard Assessment for Australia.* Geoscience Australia Professional Opinion. No.2008/04.

Gudmundsson , O. and M. Sambridge, 1998. A regionalized upper mantle (RUM) seismic model, *J. Geophys. Res.* **B4**, pp.7121-7136.

ICMMG - *see* Institute of Computational Mathematics and Mathematical Geophysics.

Johnson, R. W., 1987. Large-scale volcanic cone collapse: the 1888 slope failure of Ritter volcano, and other examples from Papua New Guinea. *Bull. Volcanol.* **49**, pp.669-679.

Keys, J.G., 1963. The tsunami of 22 May 1960 in the Samoa and Cook Islands. *Bull. Seism. Soc. Am.* **53**(6), pp.1211-1227.

Kopp, H. and N. Kukowski, 2003. Backstop geometry and accretionary mechanics of the Sunda margin, *Tectonics*, **22**, 6, 1072, doi:10.1029/2002TC001420.

Mader, C.L., 2002. Modeling the 1958 Lituya Bay mega-tsunami, II. *Sci. of Tsun. Haz.* **20**(5), pp.241-250.

Mei, C., Stiassnie, M. and D. Yue, 2005. *Theory and Applications of Ocean Surface Waves.* Singapore: World Scientific.

Myles, D., 1986. *The Great Waves.* London: Robert Hale.

Narayan, J. P., Sharma, M. L. and B.K. Maheshwari, 2005. Effects of Medu and coastal topography on the damage pattern during the recent Indian Ocean tsunami along the coast of Tamilnadu. *Sci. Tsunami Haz.* **23**(2), pp.9-18.

National Geophysical Data Centre, 2007. *Global Tsunami Database*, National Oceanic and Atmospheric Administration, Washington, viewed 23 May 2007, <http://ngdc.noaa.gov/seg/hazard/tsu_db.shtml>.

NGDC - *see* National Geophysical Data Centre.

Okal, E.A., Borrero, J. and C.E. Synolakis, 2004. The earthquake and tsunami of 1865 November 17: evidence for far-field tsunami hazard from Tonga. *Geophys. J. Int.* **157**, pp.154-174.

Song, Y.T., Ji, C., Fu, L.-L., Zlotnicki, V., Shum, C.K., Yi, Y. and V. Hjorleifsdottir, 2005. The 26 December 2004 tsunami source estimated from satellite radar altimetry and seismic waves. *Geophys. Res. Lett.* **32**, L20601, doi:10.1029/2005GL023683.

Taylor, F.W., Edwards, R.L., Wasserburg, G.J. and C. Frohlich, 1990. Seismic recurrence intervals and timing of aseismic subduction inferred from emerged corals and reefs of the Central Vanuatu (New Hebrides) Frontal Arc. *J. Geophys. Res.* **95**(B1), pp.393-408.

Thomas, C., Burbidge, D., and P. Cummins, 2007. *A Preliminary Study into the Tsunami Risk faced by Southwest Pacific Nations*, Geoscience Australia.

Wang, R., Martin, F.L., and F. Roth, 2006. Computation of deformation induced by earthquakes in a multi-layered crust – FORTRAN programs EDGRN EDCMP. *Comp. and Geosc.* **29**, pp.195-207 (inc. erratum).

Webster, M. A. and P. Petkovic, 2005. *A*ustralian Bathymetry and Topography Grid, June 2005, Geoscience Australia, Record 2005/12.

Wells, D. L. and K. J. Coppersmith, 1994. New empirical relationships among magnitude, rupture length, rupture width, rupture area and surface displacement, *BSSA*, **84**(4), 974-1002.

Wessel, P. and W. H. F. Smith, 1991. Free software helps map and display data, *EOS Trans*, AGU, **72**, 441.

Appendix A PTHA Method

A.1 Summary

The probabilistic tsunami hazard assessment undertaken in this study seeks to assess the probabilities of certain waveheights being exceeded due to the arrival of a tsunami at the locations under investigation. These probabilities are expressed in terms of expected *return periods*. This method has been used previously (for example in Burbidge *et al*, 2007, 2008) and is based on a well established method of probabilistic seismic hazard assessments. Broadly, it involves producing and analysing a very large catalogue of synthetic tsunami which is produced by combining, in various ways, a much smaller number of synthetic tsunami. The steps involved are:

1. Determine the locations at which the assessment of hazard will be made (the *model output points*, see Figure 2).
2. Create a model of the faults to be considered (that is, the location and geometry of the subduction zones under consideration, Figure 5).
3. Segment these faults into smaller fixed size subfaults. In this study, subfaults consisting of 100×50 kilometre rectangular segments were used (Figure 36).
4. Model the deformation of the sea floor produced by an earthquake involving one metre of slip on each subfault, and model the propagation of the resulting tsunami to each of the model output points.
5. Create a catalogue of synthetic earthquakes along the faults, containing values for their location, area, magnitude, and the probability that each event might occur.
6. Determine which subfaults fall within the rupture area of each synthetic earthquake, and to what extent each such subfault contributes to the synthetic event (that is, what slip should be attributed to the subfault).
7. Combine the modelled tsunami produced by each contributing subfault (from Step 4) to estimate the tsunami produced by the synthetic event.
8. Aggregate over the resulting catalogue of synthetic tsunami to determine relationships between maximum tsunami amplitudes and their probabilities.

In this study the tsunami from a total of 983 subfaults were combined in different ways to produce a catalogue of 59,871 synthetic tsunami.

More detailed information on the method used is presented below.

A.2 Bathymetry

The bathymetry was based on a combination of the US Naval Research Laboratory's two minute Digital Bathymetric Database (DBDB2) and Geoscience Australia's 250 metre dataset (Webster & Petkovic, 2005), which was resampled to a regular grid of locations spaced two arc minutes apart. This is a 'generic' bathymetry dataset and, while there are higher resolution data available for some parts of the study region, because of the very large study area it was not possible to perform the computations at a higher resolution with the

computational resources available. Two arc minutes (≈ 3.7 kilometres) is considered to be an adequate resolution for modelling the propagation of tsunami in the open ocean in deep water, and since the model output points were chosen to lie in water at least 100 metres deep (see Section A.3), for the most part the resolution will be adequate for modelling the tsunami amplitudes at those points. However there are several effects of the resolution that should be noted:

- In many nations the bathymetry is very steep so that neighbouring bathymetric grid points may fall on dry land and in water as deep as several thousand metres.
- Some very small islands may not be represented in the bathymetry at all, that is, there may be no 'dry' grid point that represents the island (see Figure 35). In such a case the semi-automatic procedure adopted for selection of model output points (Section A.3) may not place a model output point near that island, and consequently there may be some very small inhabited islands within the nations included in this study that are not represented by model output points.
- Regions of very complex and rapidly varying bathymetry may not be adequately represented by the bathymetric dataset, and in these regions the modelling of the tsunami amplitudes must be interpreted with caution. One such region is the Chuuk Islands, in the Federated States of Micronesia, shown in Figure 35. While the major islands are represented, it is unlikely that the resolution of the bathymetry in this region is sufficient to allow adequate modelling of tsunami amplitudes at points close to these islands.

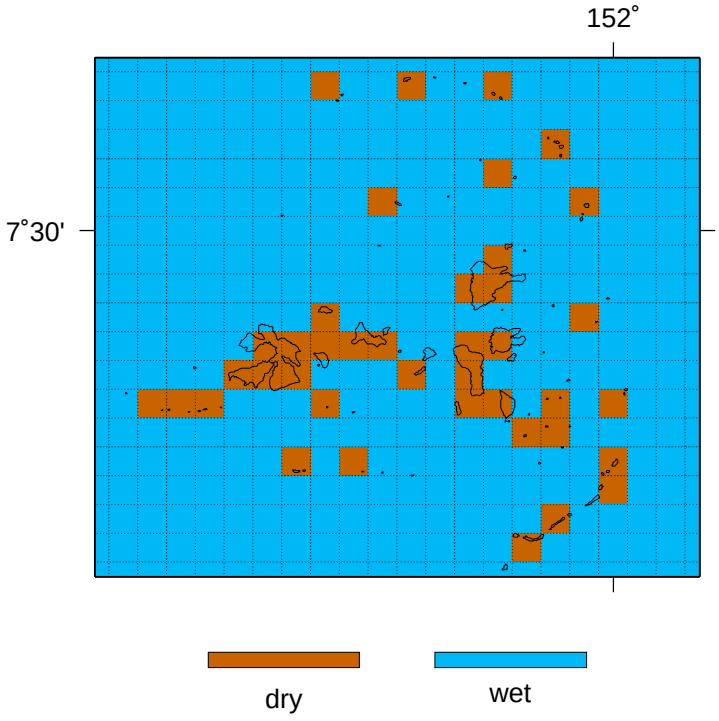

Figure 35: The Chuuk Islands in the Federated States of Micronesia. The background is the bathymetric grid used in the study, categorised into wet or dry areas. The grid lines indicate the resolution (two arc minutes) of the grid. The coastlines are overlaid using the full resolution coastline dataset available as part of the Generic Mapping Tools (GMT see Wessel & Smith (1991)).

A.3 Model Output Points

The model output points were produced by determining the bathymetric grid points that are as close as possible to each of the SOPAC nations, but at least 100 metres deep. The resulting set of grid points was thinned to reduce data volume, and edited manually to ensure that populated islands (according to the LandScan^{TM} 2004 dataset) were adequately represented. The locations of the 2875 model output points used in the study are shown in Figure 2. While the water depth at each model output point is at least 100 metres, in many cases it may be much deeper, because of the steeply varying bathymetry in the region of some of the nations in the study, and the resolution of the bathymetry data used. In order to be able to compare results from output points at different depths, Green's Law (see for example Mei *et al*, 2005) has been used to normalise all results to a nominal depth of 100 metres. Thus if z_{actual} is the modelled waveheight at an output point of depth d, then the normalised waveheight at that output point,

$$z = z_{\text{actual}} \left(\frac{d}{100} \right)^{\frac{1}{4}}$$

may be considered to be the equivalent waveheight at a depth of 100 metres if there is no focussing or de-focussing of the wave between the two points. All results in this study were expressed in terms of these normalised waveheights.

A.4 Fault Model

This was based on the plate model of Bird (2003). The dip was estimated from the Regional Upper Mantle (RUM) model of Gudmundsson and Sambridge (1998) or from papers based on seismic surveys of specific subduction zones. A map of the 983 subfaults used in this assessment is shown in Figure 36. The subfaults in this figure are coloured according to depth.

A.5 Numerical Modelling of Sea Floor Deformation and Tsunami Propagation

The sea floor deformation was calculated by representing the fault as a dislocation in a layered elastic media. The elastic properties of the crust were based on CRUST2.0 (Bassin *et al*, 2000) and Kopp and Kukowski (2003). The general method used to calculate the sea floor deformation is described in more detail in Wang *et al* (2006).

The tsunami propagation was modelled using a staggered grid finite difference scheme to numerically solve the linear shallow water wave equations.

A.6 Catalogue of Synthetic Earthquakes

The earthquake catalogue was developed using a logic tree approach. Each branch of the tree represents some characteristic of an earthquake, for example magnitude, area or depth, and has an associated probability. The tips of the outermost branches represent the synthetic earthquakes, and the probability of each earthquake is the product of the probabilities of those branches of the tree leading to that earthquake.

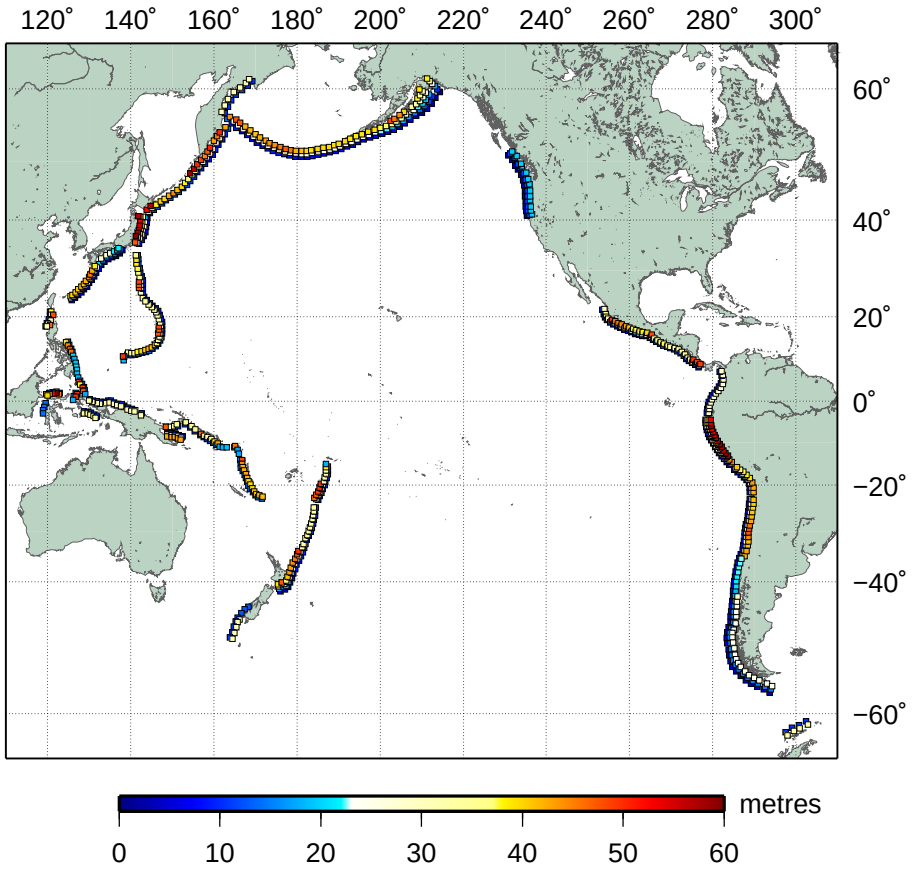

Figure 36: Location of the 983 subfaults used in the study, showing the depth of the centroid of each subfault.

Activity rates were based on the fault slip derived from plate motion rates and the length and geometry of each subduction zone. The method used is similar to the one described in Burbidge *et al* (2008) except that the variable dip of the faults was taken into consideration. The recurrence was assumed to obey the Gutenburg-Richter relation up until a maximum magnitude cut-off value that differed for each zone. For most zones four different cut-off values were used. Every magnitude between 7.0 and the maximum was modelled at increments of 0.1 magnitude units. For most modelled magnitudes, two different possible rupture areas and two different possible rupture lengths were included in the catalogue. The Wells and Coppersmith (1994) relations were used to determine the area and length as a function of magnitude. In total, 59,871 earthquakes were included in this assessment.

A.7 Deaggregating the Hazard

Deaggregation of the hazard allows the source of the hazard at a particular location to be identified, or over a region as a whole. There are a number of ways of deaggregating hazard and this section is devoted to an explanation of the methods adopted in this study.

A.7.1 Deaggregated Hazard Maps

A deaggregated hazard map allows the main sources of the hazard to be identified for a *single offshore location* for a *single return period*:

1. Choose the return period and the offshore location (model output point) at which the deaggregation is to be performed.
2. Determine the maximum expected tsunami amplitude at the chosen model output point for the chosen return period.
3. Find all events in the synthetic catalogue of tsunami that produce a wave that exceeds this amplitude at the given model output (call these the *exceedance events*), along with their probabilities.
4. For each exceedance event, find the subfaults that constitute that event and apportion the probability of the event equally among those subfaults.
5. Sum these probabilities over all the exceedance events, to calculate a probability for each of the 982 subfaults.
6. Express the results as a percentage contribution from each subfault.
7. Map these contributions.

A.8 Regional Weighted Deaggregated Hazard Maps

Each deaggregated hazard map is peculiar to the model output point for which it is produced, and indicates the source of the hazard at that particular model output point only. Thus it is possible for a deaggregated hazard map for a point on one side of an island to indicate that the main source of the hazard at that point is the Chile trench, for example, while such a map for a point on the other side of the island might indicate that the major source of hazard for that point is the Tonga trench. A regional weighted deaggregated hazard map gives some indication of the source of hazard to the region as a whole:

1. Choose the return period.
2. Deaggregate the hazard as described above *for all the model output points*, to obtain the relative contributions of each of the subfaults, for every model output point.
3. Weight the contributions of each subfault at each model output point by the maximum tsunami amplitude for the chosen return period at that model output point.
4. Sum the results over all the model output points, and express as a percentage of the total contribution.

Appendix B Validation: Kuril Islands, 15/11/2006

On 15 November 2006 a magnitude 8.3 earthquake occurred at 153.230°E 46.607°N off the Kuril Islands (Figure 37) which produced a tsunami across the Pacific with measured wave heights of (for example) 88 cm at Hawaii, 176 cm at Crescent City, California, and 57 cm at Samoa (according to the USGS). The modelling procedures used in this study have been validated against a detailed finite fault model for this earthquake published by the USGS, and data from ocean bottom pressure gauges deployed by the US Government's National Oceanic and Atmospheric Administration (DART gauges) and by the Japanese Agency for Marine-Earth Science and Technology (JAMSTEC). The locations of these gauges are shown in Figure 37.

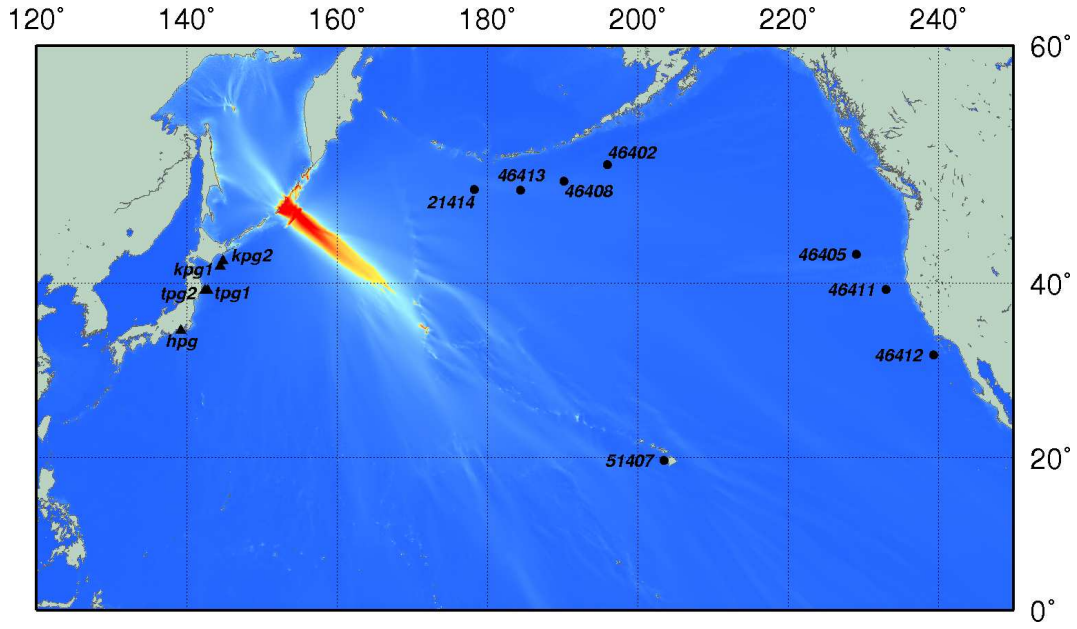

Figure 37: Numerical model of the Kuril Islands earthquake and tsunami of 15 November 2006, with the locations of the DART (circles) and JAMSTEC (triangles) ocean bottom pressure gauges.

Using the techniques discussed in Appendix A, the finite fault model published by USGS was used to compute an estimate of the sea floor deformation due to the Kuril Islands event and the propagation of the resulting tsunami was modelled. Results of the numerical simulations were calculated at the location of the ocean bottom pressure gauges for comparison with the actual water levels recorded by the gauges. It was necessary to filter the pressure gauge data to remove extraneous signals, primarily ocean tides and high frequency components that are not part of tsunami waveforms. The comparisons are presented on the following pages, with the filtered pressure gauge signals in blue and the model results in red. Overall the model results agree well with the pressure gauge data, particularly for the first peak and trough of the waveform. While there are some differences in phase, the amplitudes and arrival times are in good agreement. On average the maximum amplitudes agree to within 23%. As well as possible shortcomings in the modelling procedure (including limitations in the bathymetric model used), such differences as there are can be attributed to a disparity between the actual earthquake rupture and the USGS finite fault model, and the filtering process used for removing tidal components from the observed pressure data.

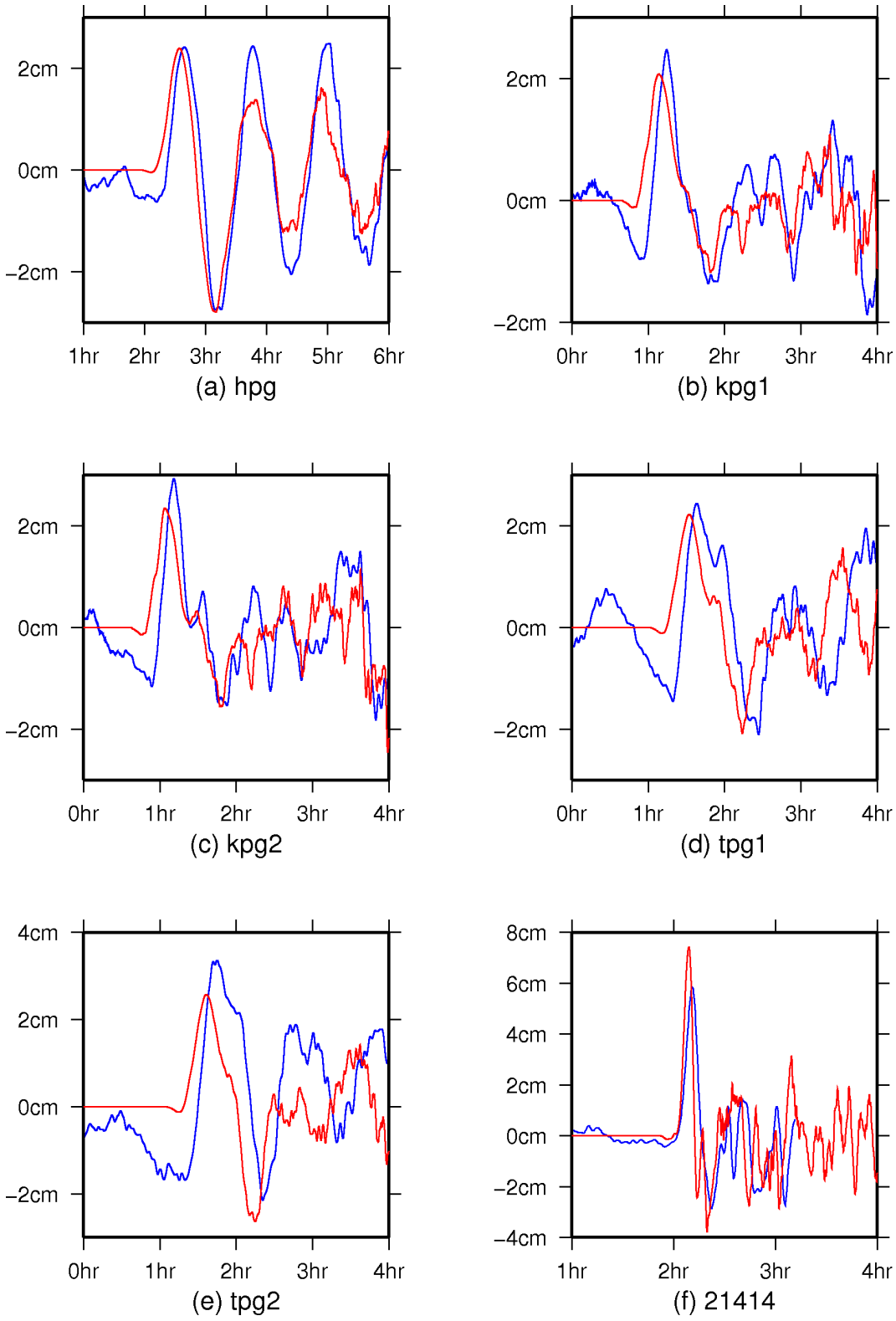

Figure 38: (a – f) Comparison of ocean pressure gauge data (blue) and model results (red) for the Kuril earthquake and tsunami of 15 November 2006.

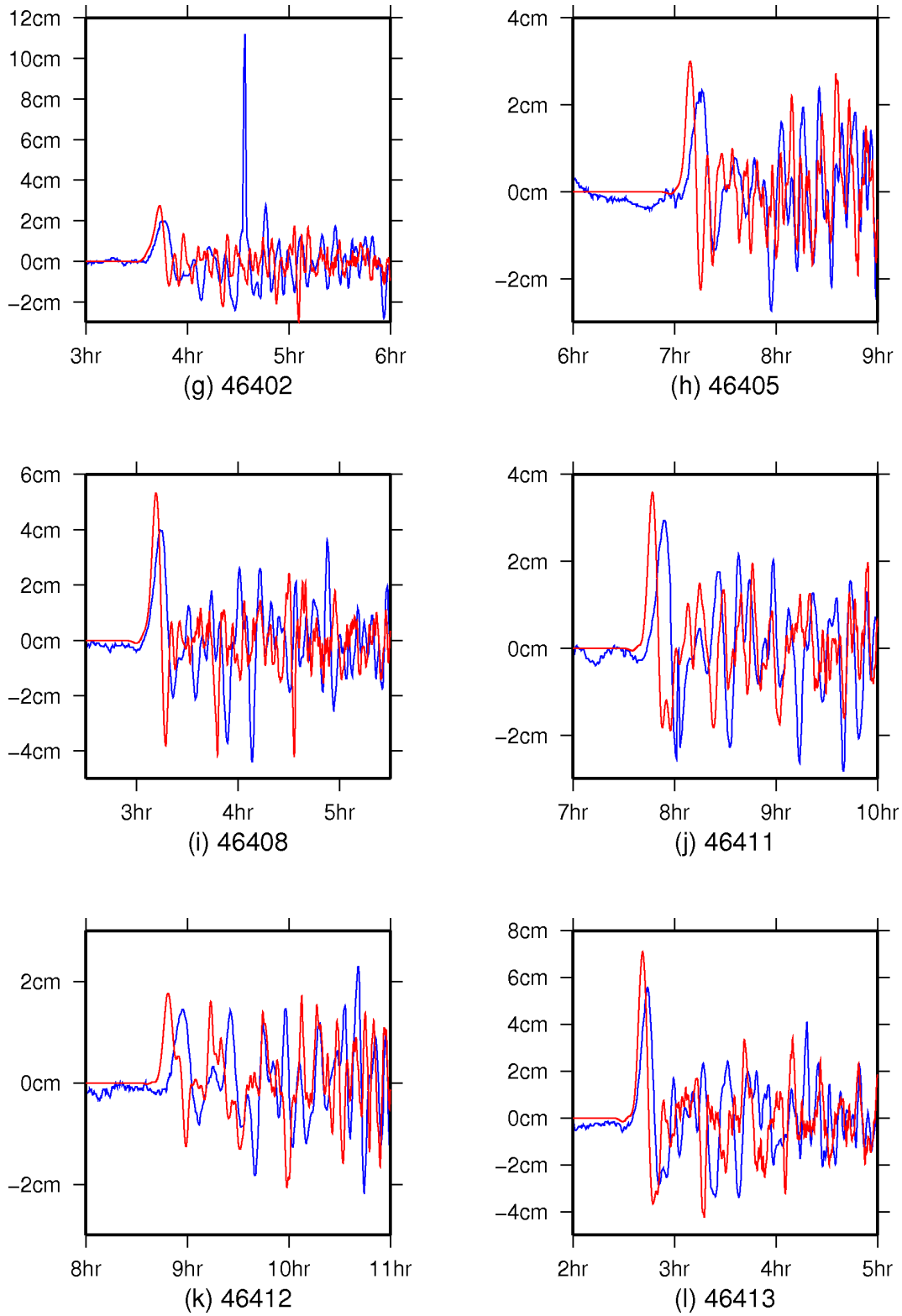

Figure 38: (g – l) Comparison of ocean pressure gauge data (blue) and model results (red) for the Kuril earthquake and tsunami of 15 November 2006.

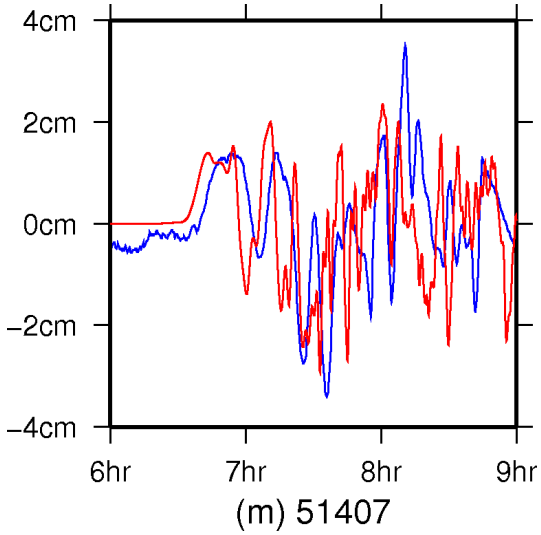

Figure 38: (m) Comparison of ocean pressure gauge data (blue) and model results (red) for the Kuril earthquake and tsunami of 15 November 2006.

The spike in the signal from DART buoy 46402 is likely to be a data error and is we believe is probably not part of the tsunami signal.

The DART and JAMSTEC buoys are in water several thousand metres deep. It has not been possible to validate the modelling procedure against data from shallower water because such data come from instruments such as harbour tide gauges that typically are in water only a few metres deep, where the model is not valid. There is some concern that the bathymetric grid resolution employed may not be high enough to always adequately represent the waveforms, particularly in shallower water where their wavelength will be shorter.

Appendix C Validation: Chile, 22/05/1960

On 22 May 1960 the largest earthquake ever recorded with modern seismographs (Mw 9.5) occurred off the coast of Chile (at approximately 286.5°E, 41°S). This produced a Pacific wide tsunami that caused widespread damage, particularly along the coasts of Chile, Hawaii and Japan.

The techniques of Appendix A have been used to estimate the sea floor deformation produced by this event and to model the resulting tsunami, based on a uniform slip model for the earthquake presented by Barrientos and Ward (1990). Figure 39 shows the results of this modelling.

In Western Samoa the tsunami was most pronounced at Fagaloa Bay (Upolu) where the maximum run-up (the highest point above sea level reached by the wave) was estimated to be about 2.5 metres (Keys, 1963). Minor damage to buildings was sustained and it was reported that the waves carried fuel drums 73 metres inland. Residents, who had been forewarned by announcements on the local radio station, had taken refuge on higher ground and no loss of life occurred. The rest of Western Samoa appears to have escaped undamaged, probably because of screening by offshore reefs, which are absent from Fagaloa Bay (Keys, 1963). In American Samoa the tsunami reached a maximum run-up height of over three metres at Pago Pago village (Allport and Blong, 1995). Buildings were moved off their foundations and a house washed into the bay. No loss of life was reported.

In Fiji reports appear to be confined to the effects in Suva harbour. The maximum runup was reported to be about 0.5 metres, and the tsunami induced a powerful surge in the harbour. Many boats sustained damage, but no loss of life was recorded (Allport and Blong, 1995).

In French Polynesia many of the islands are protected by outer reefs and deep lagoons, with rather steep bathymetry offshore, and in most cases only slight damage was sustained. No loss of life was recorded. The average runup surveyed in Tahiti was 1.7 metres. Larger runups, up to 3.4 metres, were recorded along the north shore of the island which is more exposed to the open ocean (Vitousek, 1963). The greatest effects in French Polynesia were felt in the Marquesas Islands which have few outer reefs and more gradual changes in offshore bathymetry. Runups of at least 4.5 metres (possibly up to nine metres) were observed. Destruction of buildings near the shore was reported (Vitousek, 1963).

The Hawaiian islands suffered extensive damage and 61 deaths. The island of Hawaii bore the brunt of the damage, mostly around Hilo where all the deaths and most of the damage occurred. Damage to buildings was extensive in this area, with almost total destruction in an area of nearly 300 acres. Rocks weighing up to 22 tonnes were carried 180 metres inland. There was considerable damage to houses and commercial buildings on Maui, with some being destroyed. The other islands suffered only minor damage (Cox and Mink, 1963).

In Japan, run-ups of up to 6.4 metres were recorded (ICMMG, 2006), causing widespread flooding and damage. About 5000 homes were lost leaving 50,000 people homeless, and between 180 and 190 lives were lost (Myles, 1986).

The effects of the tsunami were felt in Australia, with boats removed from their moorings in Sydney, Brisbane, Newcastle and Evans Head. Minor damage and flooding was reported in New Zealand and Papua New Guinea (Allport and Blong, 1995).

In Chile, of course, damage and loss of life were extensive. A maximum run-up of

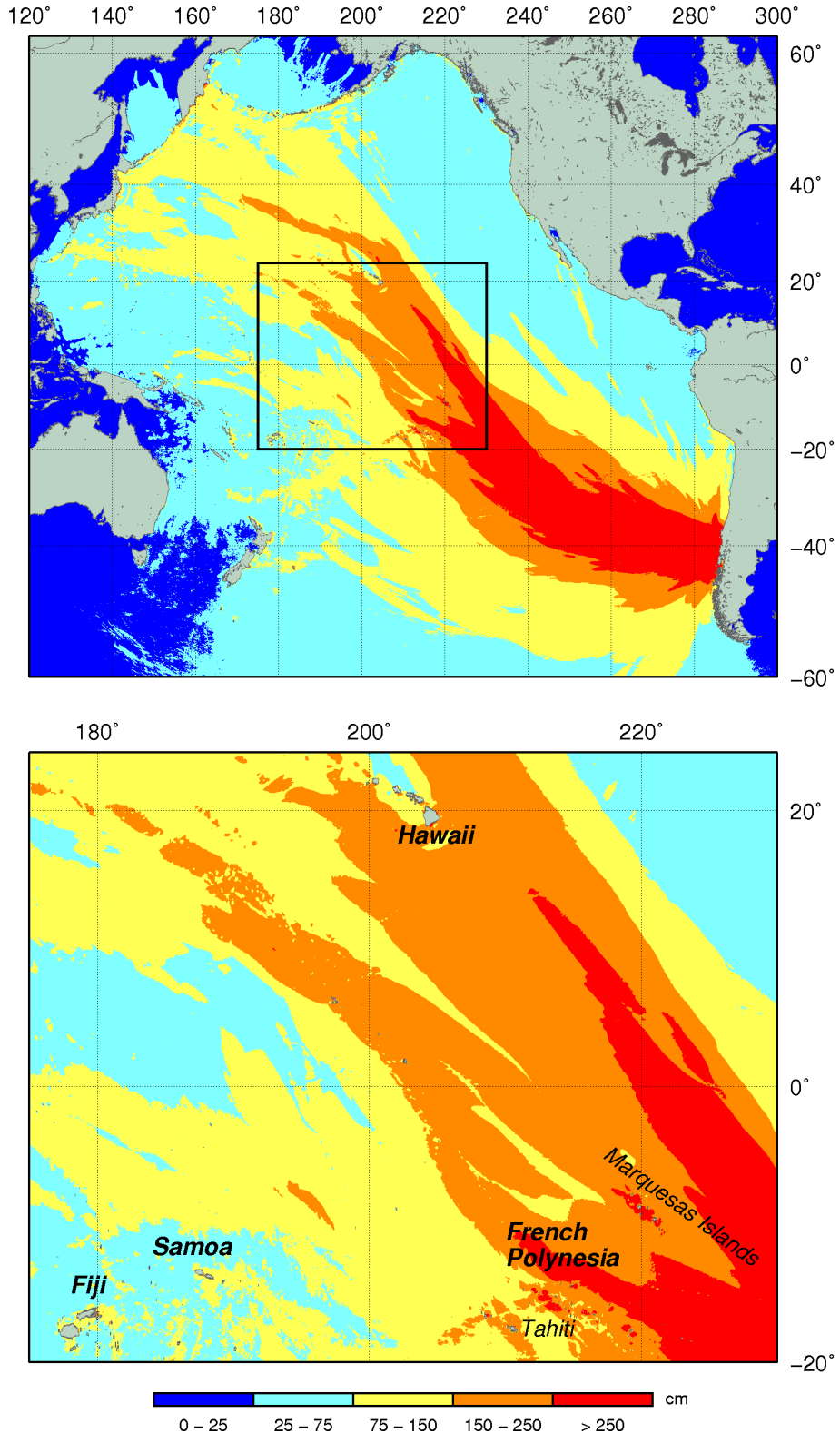

Figure 39: Normalised modelled maximum wave heights of the 1960 Chilean tsunami based on uniform slip model given by Barrientos and Ward (1990). Wave heights have been normalised to 50 metres depth and the maximum is taken over the full time period of the simulation.

25 metres was recorded (NGDC, 2007) and thousands of people drowned. Towns were completely obliterated and debris was carried more than three kilometres inland (Myles, 1986).

These historical accounts should be read in conjunction with Figure 39. Little damage and no loss of life was reported for coastlines where the incident waves had an offshore amplitude less than 0.75m (for example Australia, Papua New Guinea and, for the most part, New Zealand). However the magnitude of the effect of the tsunami was critically dependent on local features of the coastline, the height of the tide when the tsunami arrived and the density of the population in vulnerable areas. This is demonstrated by the observation that Fiji, Samoa and parts of French Polynesia received with maximum amplitudes between 0.75m and 2.5m but sustained only minor damage, whereas similar amplitude waves offsgire in Hawaii and Japan caused extensive damage and loss of life. Tsunami with offshore amplitude above 2.5m, such as those received along the coast of Chile, resulted in extensive damage and loss of life in South America but not as much in French Polynesia.